Seismic Study of Isla São Miguel, Açores

Prepared on behalf of the Laboratório de Geosciencias e Técnologia
of the Regional Government of the Açores
in cooperation with
the Instituto Nacional de Meterologia e Geofisca

by

1983

The United States Geological Survey
Office of Earthquakes, Volcanoes, and Engineering

INDEX

Tables

Introduction

In this report, we present the seismic data collected by the U. S. Geological Survey during the months of June to October, 1983 in the region of the Agua de Pau volcano, Isla São Miguel, Açores. The study was performed on behalf of the Laboratório de Geociencias e Técnologia (LGT) of the Regional Government of the Acores (RGA), in cooperation with the Instituto Nacional de Meterologia e Geofisica (INMG) Acores, as part of the LGT program to define the geothermal resources of the Agua de Pau volcano, São Miguel. LGT directly contracted the Office of Earthquakes, Volcanoes, and Engineering, United States Geological Survey to conduct the study. It is hoped that this study would form the basis for a long-term monitoring program of this volcanically and seismically active region.

Members of the United States Geological Survey from Denver, Flagstaff, the Hawaiian Volcanic Observatory, and Menlo Park have also participated in the geothermal assesment of São Miguel from 1979 to the present, under a program funded by the United States Agency for International Development (AID). Studies have included detailed geologic mapping, geochronology, hydrogeochemical sampling of thermal and non-thermal systems, geoelectrical studies, and synthesis and interpretation of the combined data sets. In their final report to AID and RGA Muffler and Duffield (1984) present a detailed geothermal interpretation of all available data sets. In this report we present seismic data collected using 10 three-component digital event recorders which were installed by the USGS to augment the 8-station INMG permanent network on São Miguel.

Geologic and plate tectonic setting.

The Açores are located along the Açores-Gibraltar Ridge which seperates the African and Eurasian plates, and extend west past the Mid-Atlantic Ridge (MAR) into the North American plate (Laughton et al, 1972). The nine islands are part of a broad plateau. The origin of the Azores Plateau has been the subject of several interpretive plate tectonic models (Figure 1). Wilson (1963) postulated the islands were formed at the MAR and as a result of sea-floor spreading and were moved to their present position. The linear northwest-southeast trend of the Acores and well resolved focal mechanisms for the magnitude 7.2, Terceira, Açores earthquake of January 1, 1980 and its aftershock sequence (Hirn et al., 1980) indicate a northwest trending tensional structure through the Açores plateau, perhaps showing that the plateau is the result of upward migration of a magmatic system through the weak zone of a transcurrent fault system. Rayleigh wave dispersion across the Açores Plateau (Searle, 1976) and rare earth studies of basalts from the Mid-Atlantic ridge onto the Acores plateau (Schilling, 1975) give evidence that the Açores plateau is a typical hot-spot above a mantle plume. K/Ar dates from the islands in the archipelago show a development of the island system from about 5.5 my to the present (Feraud et al., 1979), however, the ages of ocean floor basalts do not correspond to the ages of the islands, nor are the ages derived on the islands compatible with migration over a fixed hot spot. Searle (1980) presented side-scan sonar data from the Açores plateau and triple junction area. He postulates that the area between the mid-Atlantic ridge and the Gloria transform fault (east of the Açores) is a spreading center which accounts for the thickening of the crust in the area of the Açores plateau. The spreading rate of the Mid-Atlantic ridge relative to the North American plate is lower to the south of the Açores

than that north of them indicating a dextral transcurrent movement of 0.23 cm yr-1 along the East Açores Fracture zone (Krause and Watkins, 1970). This does not appear to be compatible with a Acores spreading center.

Isla São Miguel is located on the active Terceira Rift which passes through the Agua de Pau massif in a northwest-southeast axis (Geonomics, 1976). Agua de Pau Volcano makes up the central portion of Isla São Miguel with the volcanic centers Sete Cidades to the west and Furnas-Povoação to the east (Figure 2). The volcano is built on a complex of trachytic welded tuffs, basaltic and trachytic lava flows which range in age from 100,000 to 300,000 years b.p. The main cone consists of trachytic domes, flows and pyroclastic deposits. Carbon-14 ages from the pyroclastic flows on Agua de Pau have yielded ages greater than 40,000 years to about 4600 years b.p. The historical eruption in 1563 produced the pumice that covers most of the summit and upper flanks of Agua de Pau. Mafic lavas were erupted from the flanks of Agua de Pau in A.D. 1563 and 1652. The summit of Agua de Pau Volcano is indented by a caldera 3 kilometers wide and 100 to 300 meters deep. The caldera is uneroded, which suggests it was formed relatively recently, perhaps corresponding to the eruption at about 4600 b.p. Several pyroclastic deposits on São Miguel erupted from Agua de Pau suggest earlier caldera forming episodes (Duffield and Muffler, 1984).

Seismic Studies

Seismic studies are important for the Açores in general and for São Miguel in particular for the following reasons:

1. Earthquake hazard evaluation and monitoring
2. Volcano hazard evaluation and monitoring

3. Geothermal exploration and environmental monitoring of geothermal activities.

Earthquake monitoring

The Açores are situated at the intersection of two active seismic zones, the Mid-Atlantic Ridge and the Açores-Gibraltar Ridge (Figure 3). Reports of historical seismicity (Machado, 1965-1966; Machado, 1972-1973; and Machado and Forjaz, 1965) indicate the frequent occurrence of felt earthquakes and infrequent occurrence of destructive earthquakes in the Açores archipalago. The potential for large earthquakes in the populated islands of the Açores was demonstrated by the occurrence of the destructive Terceira earthquake (M=7.2) of January 1, 1980. Isla São Miguel was last subjected to a destructive earthquake which occurred near the town of Villa Franca do Campo in 1522. The island appears not to have had a major seismic crisis since then (Geonomics, 1977). The miles and miles of very old unbuttressed and uncemented, hand-erected stone walls that traverse the landscape of São Miguel indicate major seismic events are quite rare.

Volcano monitoring

In addition to the potential seismic risk, volcanic hazards provide a compelling reason for the seismic monitoring of all the Açores islands, and in particular, the highly populated São Miguel. The three active stratovolcanoes of Sao Miguel, Sete Cidades, Agua de Pau, and Furnas (Figure 2) have a long record of explosive eruptions. Booth et al. (1978), using tephrachronology, have documented a total of 57 volcanic eruptions during the past 5000 years in Sao Miguel. "Of the 28 trachytic and 29 basaltic eruptions known to have occurred during this period, ten were of magnitude 6, twenty-six of magnitude

5, and at least 9 of magnitude 4 or less (in Tsuya's scale based on total volumes of material erupted). ...Although no eruptions of magnitude 7 have occurred during this period, such eruptions are no doubt possible on the island. ...An eruption of magnitude 6 thus takes place on an average every 500 years in Sao Miguel, one of magnitude 5 every 200 years..." (Booth et al. 1978). The most recent eruptions were in 1562 at Fogo (magnitude 6) and in 1640 at Furnas (magnitude 5).

Even though information on the seismic activity preceding any of these eruptions is scanty, we think it is reasonable to assume that volcanic eruptions in the Açores are preceded by intense seismic activity as in other major volcanoes of the world. The 1957-1958 Capelinhos eruption on Isla Faial was documented by Machado et al. (1962). No seismic monitoring devises were located on the island at the onset of the eruption and so the pre-eruptive seismicity is unknown. A standard Bosch-Omori seismograph was installed several months after eruptive activity began and was operating during a seismic swarm in May, 1958. From May 12 to May 13, 450 earthquakes were felt on Faial, many of intensity 10 (Machado et al., 1962) on the modified Mercalli scale. The shocks were centered between the new eruptive vent and the summit caldera of Faial. In this brief period of time over 500 homes were destroyed. Hence, we believe that a continuous seismic monitoring of the Acores volcanoes is an absolute necessity. Particularly for São Miguel, a properly operating volcano monitoring system based on precise locations of seismic activity in and around the island could save lives and property in case one of the three major volcanoes chooses to erupt.

Geothermal exploration and environmental monitoring

Seismic techniques used in geothermal studies fall into two categories,

active techniques in which controlled explosions or vibrators are used to generate seismic waves, and passive techniques in which earthquakes are used as the sources. Active studies are mainly concerned with modeling the fine structure of the crust using refraction and reflection surveys and will not be discussed in this report. Passive studies mainly consist of microearthquake surveys to establish a seismo-tectonic framework of the geothermal area under investigation and to model the three-dimensional structure of the area. Seismic waves from local, regional, and distant earthquakes can be used to model anomalous physical properties of the underlying rock such as those caused by hydrothermal activity or partial melting. We now give a brief review of the application of passive seismic methods in geothermal studies.

Microearthquakes. Microearthquake studies in geothermal areas can be divided into several categories: exploration, tectonic evolution, detection of zones of anomalous physical properties in the upper crust due to the presence of geothermal reservoirs, magma pockets etc., and environmental monitoring.

Exploration. Geothermal prospects are invariably located in areas of active tectonism and hence it is not surprising that most of them are seismically quite active. Ward and Jacob (1971) showed how a microearthquake survey can be used as a geothermal exploration tool to delineate fracture zones which provide paths for hot water to reach the surface. There have been numerous microearthquake surveys in geothermal areas, but no definitive results useful for geothermal exploration have so far been reported (Ward and Bjornsson, 1971; Klein et al., 1977; Marks et al., 1978; Walter and Weaver, 1980).

lectonic evolution. Whether microearthquake surveys are useful to locate geothermal drill-holes or not, their study forms an important and integral part of the process of understanding the volcanic and tectoic evolution of geothermal areas. Clear examples are provided by studies at Brawley, Imperial Valley and in the Coso geothermal area, California (Weaver and Hill, 1979). In both these areas it has been demonstrated that the geothermal zones occur at miniature continental spreading centers. There are numerous seismicity studies which provide detailed information on the volcano-tectonic evolution of geothermal areas on a macro and micro scale.

Detection of zones of anomalous physical properties. Microearthquakes can be used to look for velocity and attenuation anomalies associated with hydrothermal reservoirs and magma pockets in geothermal areas. Chatterjee et al., (1984) found abnormally low Vp/Vs (and hence Poisson's ratio) beneath the geyser basins of Yellowstone National Park, Wyoming. They attributed this to the presence of hydrothermal reservoirs in which the temperatures were close to those needed for the transition of water to steam. Sanders and Ryall (1983) used the observed strong attenuation of S-waves from microearthquakes along certain paths to map the subsurface geometry of magma bodies in Long Valley, California. In the same region, Kissling et al. (1984) using local earthquake data and a tomographic inversion method have delineated a zone of low P-wave velocity in the depth range of 3 to 7 km beneath the resurgent dome and the south moat of the Long Valley caldera.

Environmental monitoring. In general, seismic activity occurs in many geothermal areas of the world. Ward (1972) has discussed the problem of earthquake risks associated with geothermal activity. One main concern is

whether the extraction of fluids and reinjection of spent fluids could trigger a moderate earthquake. There is clear evidence that modifying fluid pressure can alter the seismicity pattern in an area. Also, seismic activity seems to be triggered by injection of fluids at high pressure into the ground (Healy et al., 1966; Raleigh et al., 1976). Eberhart-Phillips and Oppenheimer (1984) showed by careful relocation of earthquakes in the Geysers geothermal area, California, that seismic activity tends to cluster near production wells in the steam field. They could not find statistically significant results to show whether seismicity was indeed induced by the reinjection of spent fluids. They postulate that the seismic activity associated with geothermal production could be a result of perturbation of the regional stress field due to volumetric contraction caused by steam withdrawal.

Regional earthquakes and teleseisms. An important constituent of a geothermal system is the heat source that activates it, usually some form of magmatic intrusions. In order to estimate the longivity of the geothermal system and to understand its volcanic setting, it is important to detect and delineate these magmatic intrusions. The technique of measurement of teleseismic residuals has been successfully used to make three-dimensional models of velocity anomalies in the crust and upper mantle of the earth (Aki, 1982) and has been used by Iyer et al., (1979,1981), Reasenberg et al., (1980), Robinson and Iyer (1981) and Steeples and Iyer (1976), to map magma chambers in several geothermal areas in the United States. (For a review of geophysical detection of magma chambers, see Iyer, (1984). Even though no case histories are available, regional earthquakes can also be used in a similar way to locate anomalous low-velocity zones in the earth's crust.

Previous work in Sao Miguel

As part of the geothermal exploration and development program which was begun in 1976 in São Miguel, many varied geologic and geophysical studies have been undertaken by LGT, private contractors, and the USGS (Geonomics, 1976; 1977; Gandido et al., 1984; and Muffler and Duffield, 1984). Prior to 1976 the scientific work on São Miguel was restricted to studies of geologic processes and volcanic histories. Geologic accounts of São Miguel are given by Branco et al. (1957), Jerimine (1957), Zbyszewski (1961), Assunção (1961), Walker and Croasdale (1971), and Booth, Croasdale, & Walker (1978). Volcanic activity has been documented by Weston (1964) and Machado (in Van Padang et al. 1967). The tectonic setting of the Açores has been discussed by Krause and Watkins (1970), Laughton et al. (1972), Feraud, Kaneoka, and Allegre (1979), and Searle (1980). In 1973 a research hole was drilled by scientists from Dalhousie University to obtain information on the volcanic stratigraphy on the north side of Agua de Pau. Temperature gradients measured in the hole were in excess of 200°C at depths greater than 500m (Muecke et al. 1974).

The first microearthquake survey was conducted in São Miguel by Geonomics (1977) in the Agua de Pau geothermal prospect and surroundings. However, the survey lasting about 8 weeks using a portable seismic network, yielded only 11 locatable seismic events and has not provided any useful information, geothermal or otherwise. Subsequently, LGT in collaboration with INMG has set up a 8-station seismic array in São Miguel. The data from this network has not yet been plotted or interpreted.

Plan of the Paper

Instrumentation, earthquake location and magnitude determination procedures, temporal and spatial patterns of seismicity, Vp/Vs ratios, and analysis of residuals from regional earthquakes will be discussed. Appendices A, B, C, and D list respectively, clock corrections, HYPO71 input parameters, symbol explanations , earthquake origin times, epicenters and focal depths, local magnitudes, and quality of the locations.

Instrumentation and Field Work

We used 10 Sprengnether DR-100 portable digital event seismographs and two Teledyne Geotech portable drum recorders (Portacorders) for the study. Six of the digital recorders were installed around the Agua de Pau massif, three at the INMG observatory in Ponta Delgada to record 8 vertical and 1 horizontal channels of the permanent network (INMG) stations, and the tenth instrument was used as a backup and for special tests. The station names and locations are shown Figure 4 and the operating parameters are listed in Table 1.

The DR-100. The Sprengnether DR-100 is a precision 12-bit transient event recorder for signals in the frequency range 0-300 Hz and can record up to three components of seismic data. The DR-100 has an adaptive trigger system and a solid state memory to preserve signal onsets. Only channel one is used to activate the trigger. The signal from this channel is rectified and integrated in two averagers giving short-term (STA) and long-term (LTA)

Table 1

Station Names and Locations

Operating Parameters

Code	Station	Period of Operation (Day/Month/Year)	Latitude (Deg Minutes)	Longitude (Deg Minutes)	Elevation (Meters)	Seismometer Model	Gain (DB)
ADA	Agua de Alto	22/06/83 - 12/07/83	37 43.85 N	25 28.59 W	190	S-6000	66
ADB	Agua de Alto B	12/07/83 - 09/10/83	37 43.98 N	25 28.62W	200	L-4C	60-66**
CHC	Charcoal	18/06/83 - 06/10/83	37 45.92 N	25 30.59 W	632	L-4C	66
CML	Pico Cigarreiro	21/06/83 - 12/10/83*	37 46.25 N	25 32.76 W	291	S-6000	42
CRA	Cumieira	24/06/83 - 06/10/83	37 45.19 N	25 28.13 W	667	L-4C	66
EPD	Espraiados	22/06/83 - 25/07/83	37 47.72 N	25 23.81 W	506	L-4C	66
EPE	Espraiados	25/07/83 - 07/10/83	37 47.73 N	25 23.76 W	501	L-4c	66
FAC	Faja de Cima	18/07/83 - 12/10/83*	37 46.39 N	25 39.03 W	191	S-6000	42
FRA	Pico dos Cedros	21/06/83 - 12/10/83*	37 44.56 N	25 21.20 W	557	S-6000	42-48
LFA	Logoa do Fogo	21/06/83 - 12/10/83*	37 46.36 N	25 28.99 W	693	S-6000	54
LGD	Lagoa do Congro	22/06/83 - 07/10/83	37 45.27 N	25 24.37 W	454	L-4C	66
MTS	Monte Escuro	21/06/83 - 12/10/83*	37 46.86 N	25 26.31 W	826	S-6000	54-60
PFM	Porto Formosa	23/06/83 - 30/09/93	37 48.33 N	25 25.66 W	345	L-4C	66-72
PST	Pasto	20/06/83 - 06/10/83	37 44.16 N	25 31.66 W	265	L-4C	66
PVM	Pico Vermelho	18/06/83 - 23/06/83	37 47.93 N	25 30.93 W	100	L-4C	66
PVN	Pico Vermelho	23/06/83 - 06/10/83	37 47.93 N	25 30.93 W	100	L-4C	60-66**
RIB	Cerrado Novo	21/06/83 - 12/10/83*	37 47.97 N	25 27.66 W	526	S-6000	54
RIBN	Cerrado Novo	18/07/83 - 12/10/83*	37 47.97 N	25 27.66 W	526	S-6000	48
SBA	Santa Barbara	02/10/83 - 12/10/83	37 47.89 N	25 31.00 W	110	L-4C	66
SVA	Pico Gafanhoto	18/07.83 - 12/10/83*	37 47.63 N	25 19.03 W	644	S-6000	48
VIF	Miradouro	21/06/83 - 12/10/83*	37 44.69 N	25 26.38 W	647	S-6000	54

* INMG permanent stations: high cut filter 10Hz low cut filter 0.5Hz anti-alias 50

** Portable drum ink recorders

All other stations operated with high and low cut filters out; anti-alias 50

average signal levels. STA and LTA settings can be varied. The ratio of these voltages is taken and compared to a user-specified trigger threshold. When the threshold is reached the recorder is turned on. LTA is held until the STA and L1A ratio falls below the trigger threshold, and then the recorder is turned off. Pre-trigger data is stored in the shift-register memory. We used a sample rate of 100 samples/sec and pre-event memory of 3 seconds for all stations except CRA and two of the recorders (MI1 and MI2) kept in the INMG observatory which had extra memory cards and pre-event memory of 7 seconds. The DR-100 has a clock with day/hr/min/sec display derived from a Vectron TCXO, 1 MHz, oven- controlled oscillator. The system stability is : aging = $2x10^{-9}$ ppm, temperature stability $3x10^{-7}$ sec/deg from -0 C to 50 C. After the system triggers on an event, offset voltages are added to samples at subsequent odd seconds on all channels until the trigger turns off. Before each event is recorded a time code is written containing the system display information including the first odd second offset after the system trigger; after each event is recorded a time code is also written containing the system display including the last odd second offset after the system trigger. The triggered digital data including the time codes and pre-event data are recorded on cassette tapes. The recording duration for each event was about 20 seconds and therefore, each tape could hold about 20 events.

The six digital recorders installed on Agua de Pau utilized one vertical and two horizontal L-4 1-Hz geophones and 5-pole low-pass filters set at 50 Hz. Gains for the field instruments ranged from 42db to 72db. The seismometer response and the total system (seismometer - filter - DR-100) response are shown in Figure 5. The operating variables changed with each instrument depending on the site location and level and type of cultural

noise. Our tenth recorder was used as a backup and was operated briefly with a borehole seismometer to test the variation of cultural noise with depth.

A DP-100 playback unit and paper chart recorder were also taken to Ponta Delgada to make analog playbacks of the seismograms. Some of the larger local events were timed, using the P-phases hand picked from the strip charts. We used a HP-85 microcomputer with an extra 16k RAM module and a computer program called HYP85 (similar to the computer program HYPOINVERSE) to locate earthquakes as soon as the tapes came off of the DR-100's.

The Portacorders. Two Portacorders were operated to provide visual checks of seismic activity and to obtain seismic data for sites too noisy for triggered digital recorders. They utilized L-4 1-Hz geophones, and generally were operated at gains of 60-72 db.

Timing. Two master time clocks (Master Clock II, built by the USGS) were hand carried to the Acores from Menlo Park, California to provide accurate international time standards for the experiment. The clocks contain an oven-controlled oscillator (aging = 5×10^{-10} ppm, temperature stability = 6×10^{-9} sec/deg from -40 C to +55 C) and were calibrated to the Rubidium time source in Menlo Park, California before leaving for the Acores. Once in Ponta Delgada one clock was kept stationary for the duration of the experiment and the other clock was used in the field to calibrate the DR-100 clocks and note the drift rates at every tape change. The field master clock was calibrated and reset to the stationary master clock once a day. On October 7, 8, 9, the master clock was compared to the DCF radio time code six times. The master clock drifted 41.75 ms in 110 days, an average drift rate of 0.357 ms per day (slow compared to the DCF signal).

Site Selection

Finding appropriately quiet sites for the portable stations was difficult. Nearly all of Sao Miguel is under heavy cultivation; where the terrain prohibits farming, cattle are grazed or lumbering operatons are present. Pyroclastic flows cover most of the island and rock outcrops are rare. Most of the rock outcrops occur in canyons, stream beds, along the coast, or in road cuts and for the most part are inacessible or seismically noisy. Hence, our seismometer sites were based on compromise between accessibility and best available noise conditions. They were poor quality-wise in comparison with sites for similar studies in the U.S.A.

The INMG permanent network

The INMG network on Isla Sao Miguel is centered on the Agua de Pau massif with signals from all stations telemetered to the observatory in Ponta Delgada where they are decoded and recorded on paper charts moving at a speed of 2 mm/s. The network utilizes Geotech S-6000, 2 Hz geophones. We monitored the INMG network with three of the Sprengnether DR-100's at system gains of 36 to 54 db. We recorded all vertical components and one horizontal component (Station RIB) from the permanent network. The three recorders at INMG were triggered simultaneously by channel one of instrument one (usually station VIF). The INMG recorders are set at low gain levels (24-36 db) because of the extreme cultural and natural noise levels on Sao Miguel. Because of this and the limited dynamic range of paper recordings, very few of the events recorded by our DR-100 monitors were visible on the corresponding paper recordings. The 2-Hz seismometers and 10-Hz low-pass filters in the observatory seismographs determined the system pass-band for these permanent network stations.

Data

During the recording period from June 19 to October 10, 1983, 59 locatable earthquakes, 30 to 40 unlocatable events with arrivals at only two or three stations, 300 to 325 one station triggers (quite seismic in character but very small in magnitude), and well over 200 one station events associated with swarm activity on September 6-7, 1984 were recorded. Of the 59 located events 15 are considered regional events (10 km to 140 km outside of the network). The 44 remaining events occured within network. No teleseisms were recorded, probably because of the high background noise level.

Magnitude Determination

Local earthquake magnitudes can be determined in two different ways: (1) using coda duration, and (2) using standard Wood-Anderson seismometers or by converting the digital seismograms into equivalent Wood-Anderson seismograms.

Coda Duration. In the first method, the coda-duration magnitude (M_D) is derived by computing the duration of ground motion employing the relation $M_D = a + b \log(\tau) + c\Delta$ where (τ) = the geometric mean of the total signal duration at all stations recording the event, and Δ = the arithmetic mean distance in kilometers from the epicenter to the recording statons (Lee et al., 1972). The duration is defined as the time measured in seconds beginning at the first motion and ending when the signal is lost in the background noise. In the absense of any magnitude scale for the Acores, we have used the constants in the scale for California derived by Lee et al., 1972 given as $M_D = -0.87 + 2.00 \log(\tau) + 0.0035\ \Delta$. Therefore the M_D values we present give only relative magnitudes for the Sao Miguel area. We used 20 second

recording durations including approximately 3 or 7 second pre-event memory, and so only events of less than 13 to 17 seconds duration can be used for the coda-duration method. It happened that most of the microseismicity we recorded in Sao Miguel was of 10 to 15 seconds duration . Bakun (1984) has shown that a close correlation exists between M_D and the local magnitude M_L (Richter, 1935) for the range $1.5 \leq M_L \leq 3.25$ so we feel that the M_D values we obtained give a good first approximation of the local seismic magnitudes on São Miguel. To develop a magnitude scale that is relevant to the Acores region, many more events have to be recorded, including larger magnitude local events.

Wood-Anderson Seismograms. Another method of magnitude determination consists of converting the digital seismograms to equivalent Wood-Anderson seismograms and measuring the peak amplitude directly, thus deriving M_L (local magnitude). Because of the small range of apparent magnitudes of the events recorded, we feel that the coda-duration method of determining relative magnitudes is a good first approximation of local magnitudes on Sao Miguel. A larger data set for a wide range of magnitude levels needs to be collected before a detailed analysis of local magnitudes and seismic moments can be performed.

Earthquake Location Procedures

Data from the DR-100 cassette tapes were read onto the USGS UNIX system using programs supplied by the University of Washington (UW). UW programs Ping and Salvage were used to obtain accurate timing and phase picks of the seismograms, and program Watt allowed the display of all seismograms for each event (Figure 6).

The phase data for each instrument (universal time of the first arrival,

first motion, S-arrival, and coda duration) were then entered into event files. Clocks on each instrument were checked at every tape change and reset to the master time clock. Corrections for clock drift were made for each event assuming linear drift for the clocks, and added to the picked arrival times. Appendix A is a list of clock drifts for the experiment. Earthquake locations were obtained using the computer program HYP071 (Lee and Lahr, 1975). Program parameters used are listed in Table B. Both P-wave and S-wave phases were used in the locations when the S-wave phases were clearly distinct. Several of the locations for events recorded only by INMG vertical geophone stations use only P-arrivals. Improved hypocentral solutions (lower root-mean-square (RMS) travel-time residuals and smaller standard errors) were obtained when clear S-wave phases were included in the solution (using horizontal components from the USGS stations).

Velocity models. A key element for accurately locating earthquakes is the velocity model. In the absence of available velocity models for São Miguel, we used an initial velocity model based on refraction data in the Mid-Atlantic Ridge area by Le Pichon et al., (1965) for preliminary locations while in the Acores using a minicomputer. Table 2 shows the crustal velocity model and Figure 7 is a plot of the epicenters of local events obtained with this model. We relocated all events using a crustal velocity model (Table 3) based on refraction data by Senos and Nunes (1980). We then revised their model slightly and derived a final velocity model (Table 4) with the program VELEST 2, using a linear inversion method developed by by Crosson, 1976 (Ellsworth, 1977; Ellsworth and Roecker, 1981) .

Depth (km)	Velocity (km/second)
0.00	4.50
3.80	6.80
8.00	7.50

Table 2. 3-layer crustal velocity model. (Le Pichon et al., 1965)

Depth (km)	Velocity (km/second)
0.00	2.40
0.50	4.10
2.20	5.40
5.40	6.80
11.00	7.80

Table 3. Crustal velocity model based on refraction work by Senos and Nunes (1976)

Depth (km)	Velocity (km/second)
0.00	3.20
2.20	5.40
5.40	6.20
11.00	8.16

Table 4. Final crustal velocity model. (VELEST 2)

Station	Elevation (m)	Delay
PVN	100	0.14
FAC	191	-0.10
ADB	200	0.15
CML	291	0.02
PST	265	0.08
PFM	345	-0.16
LGD	454	0.06
EPE	501	0.15
EPD	506	0.15
RIB	526	0.01
FRA	557	-0.01
CHC	632	0.24
SVA	644	-0.01
VIF	647	-0.04
CRA	667	-0.06
LFA	693	-0.07
MTS	826	-0.06

Table 5. VELEST station delay terms.

Velocity modeling using VELEST 2. Program VELEST 2 is used to simultaneously invert for selected hypocenters, a velocity model and staton corrections. 31 of the best local events were used in the VELEST 2 inversions based on two criteria for their selection: (1) sharp, clear, unambiguous P arrivals at as many stations as possible, and (2) a good distribution of hypocenters within the area of the network with as great depth variability as possible.

Initial inversion runs were made on a 12 layer model with layer boundaries arbitrarily set at 1 km intervals. The starting velocity model was chosen arbitrarily, velocity increasing monotonically with depth. The initial hypocenters were those calculated with the crustal velocity model derived by Hirn (1980). Station FRA was given a station correction of 0.00 sec and was held constant for all runs. The resulting velocity model from the initial runs indicated that the 12 layer model was unstable because, (1) the surface layer was poorly constrained, and (2) the model never stabilized or converged.

Several computer runs were then made with various layer thicknesses and numbers of layers, and it became quite apparent that all models with more than five or six layers would not converge to a final solution. Depending on the starting velocities of the model used all of the computed models did settle on one defined structure with a clear basic feature consisting of a strong boundary between 2 and 3 km depth with velocities in the range of 2 to 5 km/sec.

In the final model, the two upper layers from Senos and Nunes' model were combined into one layer with an intermediate velocity, resulting in better resolution of the upper layer. The upper mantle velocity used in the final model is taken from Whitmarsh (1973). The station residuals (Table 5) derived from the inversion give negative values indicating earlier arrivals at stations at higher elevations. This result is different from the residual

pattern obtained using regional events. We attribute this to the instability of the VELEST model. This interpretation, however, is tentative because the inversion and the resulting station residuals are not well constrained because no shots or earthquakes of known origin or detailed refraction work were available to provide known travel times for the inversion. Because of the lack of hypocenters of events at depths greater than 10 km the resolution of layers below about 5 km was always poor. Also, it was found that the number of earthquakes (31) used in the inversion and the small geographic area in which they occurred caused a trade-off between the velocity model and the station correction terms. Due to the limited data set used in the VELEST inversion and resulting small number of data points at each of the stations, we were not cnfident enough to use the VELEST station residuals for the earthquake locations. Final station delay terms which were used in the location of the local and regional earthquakes were derived using the regional earthquake residuals. The method is explained in the station residuals section, page 24. It should be noted that the velocity model obtained is representive only of central Sao Miguel as no regional events or events from outside of the network were used in the inversion.

In summary, we used three models to locate earthquakes in São Miguel: (1) the model from Le Pichon et al. (1965); (2) the Senos and Nunes (1976) refraction model; and (3) the VELEST model. The simple three-layer model from Le Pichon et al. used for prelimanary locations while in São Miguel does not take into account the thickening of the crust in the Açores Plateau or the expected slow velocities from surficial pyroclastic deposits. The model based on several refraction lines in São Miguel indicates the presence of several kilometers of thick seismically slow material at the surface. The VELEST model takes into account the slow velocities observed by Senos and Nunes but

consolidates the first two layers of his model with an intermediary velocity. The station terms help correct for elevation and local surficial conditions.

The three models all provide comparable earthquake locations, presumably due to the small spatial network and the limited depths of the events. Figure 8 is a spatial plot and corresponding depth cross-section along line A-A' of selected epicenters from the three models. The variation in epicenteral locations between the models range from 0.60 km to 3.80 km. The variation in depths (hypocenteral locations) range from 0.47 km to 3.89 km. Average RMS values are lower and hypocenter confidence levels for the local events are higher using the VELEST model and plane wave station terms.

Microearthquakes

During the period of our survey from June 18 to October 10, 1983, 44 local events in the magnitude (M_D) range of 0.6 to 2.32 were located. The hypocenters have an average horizontal modal standard error of 1.30 km, and a depth modal standard error of 1.56 km. The quality (Q) of the 44 local earthquakes as defined in appendix B is as follows:

Q	Number	Percent
BC	7	16
CC	28	63
DC	9	21

Figure 9 is the final spatial plot of earthquake epicenters (based on VELEST model and station terms using regional events) on central Sao Miguel. Appendix C contains the symbol explanation for Appendix D, the final earthquake locations and related location parameters.

Focal Depths. The focal depths of earthquakes in the Agua de Pau region

(Figure 10) range from less than 1 km to about 12 km with only two events deeper than 10 kilometers. The events have a bimodal distribution with one zone from 1 km to 3 km (partly due to the starting focal depth of 3 kilometers and poor focal resolution) and another zone from 4 km to 7 km The largest events with well constrained focal depths occurre between 2 km and 6 km.

Temporal Patterns of Seismicity. 95 percent of the locatable local events occurred on the east slope of Agua de Pau and in the topographic low between the Agua de Pau and Furnas volcanoes. This includes the area bounded by Lagoa do Fogo on the west, to Lagoa de S. Bras and Lagoa do Congro on the east. During the experiment there were approximately 7500 station triggers, and analog seismograms were made for each triggered event at all stations to determine if the triggers were culturally induced or seismic in character. We estimate that 90% of the 7500 triggers were culturally induced. Figure 11 is a plot of seismic triggers versus time for the duration of the experiment. Temporal patterns are accented by two periods of swarm activity on June 28-29, and September 6-7, 2983 with 50 percent of the located events occurring during the swarms. Locatable events averaged one event every seven days except during the swarms. However, microseismic activity was quite high during the entire recording period with several one or two station triggers occuring per day caused by events of $M_D > 1$.

Swarm Activity. The periods of swarm activity within the seismic network occurred on June 28-29 and September 6-7, 1983. The swarm activity of June 28-29, 1983 lasted for 28 hours, with eight events located during that period. The events range in magnitude from M_D 1.05 to M_D 1.50, with little associated one and two station triggers caused by smaller events during

the swarm. Paper records from station PVN and INMG showed little such activity and the digital recorders did not run out of tape as would by the case if persistent microseismicity was present. This suggests that numerous small microseisms did not accompany the swarn activity or that the noise conditions during that time were high enough to mask such events. Figure 12 is a plot of earthquake locations for the June 28-29 swarm.

The seismic swarm on September 6-7, 1983 was of a very different character. Natural noise levels were very low and most stations were running with higher than normal gains, especially the INMG station VIF. Over 200 events were recorded by station VIF during the 16-hour period from 1500 September 6, to 0700 September 7, 1983. The digital instruments closest to the swarm area triggered on the numerous events at the beginning of the swarm and ran out of tape before the larger shocks of the sequence occured. Digital recorders further than 5-6 km from the swarm triggered only on the larger events. Altogether digital records of at least 64 of the swarm events were recorded. Many of the triggers were only one or two station triggers and the INMG paper records were not clear enough to pick reliable arrivals for the small events. 23 events were large enough to be located, 11 by digital records alone, 6 by digital and paper records, and 6 by paper records alone. Figure 13 is a plot of the 23 events located during the September 6-7, 1983 swarm. The swarm began with numerous small events recorded just above the background noise level, increasing in magnitude and rate of occurrence for eight hours with at least 146 events recorded during that period, until 2310, when a M_D 2.07 event occurred. Seismic activity dropped off significantly after the 2310 event with 75 events occurring through 0600. At 0555 September 7, 1983 the largest locatable event of the swarm was recorded at M_D 2.32.

Two more locatable events were recorded at 0606 and 0635. Digital instruments and paper recorders showed that seismic activity was very low for three days after the swarm with no events recorded until September 11, 1983. Figure 14 is a plot of total events versus time for the swarm activity. Appendix E is an example of the digital station triggers during the swarm activity of September 6-7, 1983. Figure 15 is a plot of magnitude versus time for both the June and September swarms. There is no pattern discernable in the June plot while a definite trend of increasing magnitude with time is seen in the September activity.

Regional Earthquakes

During our four month experiment 15 earthquakes, presumed to be regional earthquakes were recorded. Since these events occurred well outside our seismic network, their epicenters and depths could not be determined with a high level of confidence. Among these fifteen events, six were not locatable because of lack of adequate number of P-arriveals. There were no identifiable S-phases and the emergent P- picks gave erroneous locations within the network. A typical regional event which was located using good arrivals is shown in Figure 16. Figure 17 shows the epicenters of the nine located regional earthquakes. It is interesting to note that the epicenters occur within a broad area about São Miguel with a suggestion of northwest trending alignment. A similar pattern is observed in the plot of regional seismicity from the past ten years in the Açores plateau region (Figure 3).

Vp/Vs and Poisson's Ratio

In the hypocenter location (HYPO 71) program, a constant Vp/Vs ratio is assumed and since only the crustal P-velocity model is specified, the

S-velocity is implicitly assumed to be $1/\sqrt{3}$ of P-velocity, corresponding to a homogeneous, isotropic medium. However, significant Vp/Vs variations have been found in active geothermal areas, such as Yellowstone National Park, Wyoming (Chatterjee et al., 1984), and are explained as due to the presence of pore fluids and steam filled fractures in geothermal reservoirs. We therefore considered it would be useful to estimate Vp/Vs values to look for such variations in the São Miguel Agua de Pau geothermal area.

Vp/Vs can be determined by using the Wadati method in which arrival times of P- waves (tp) are plotted as the abscissa and the difference of arrival time between the P and S-phases (Ts-Tp) as the ordinate. If Poisson's ratio (σ) is constant along the travel path of the seismic ray, the relation (Ts-Tp) versus tp will be a straight line with a slope equal to (Vp/Vs)-1 (Wadati, 1933; Kisslinger and Engdahl, 1973). Alternately, we can plot a modified Wadati diagram in which instead of plotting Ts-Tp versus Tp, the P- travel time tp is plotted as abscissa against the S- travel time ts as ordinate. Earthquake location and origin time errors are elimiated in both the methods if the Poisson's ratio does not change in the volume sampled by the seismic rays. The slope of the line through the tp versus ts travel time plot directly gives Vp/Vs. The advantage of the latter method is that travel time data from several earthquakes can be plotted simultaneously to derive an average Vp/Vs ratio for the study area. Poisson's ratio is given by

$$\sigma = 1/2((Vp/Vs)^2-2)/((Vp/Vs)^2-1).$$

Local events. We chose to use the modified Wadati method of plotting tp versus ts to derive a Vp/Vs ratio for the local events rather than the standard Wadati method for the following reasons. There were 216 P-arrivals and 151

S-arrivals for 37 well recorded local events. Of the S-wave picks, 84 were considered to be accurate and 36 were from horizontal components. However, most of the individual local events had less than 4 reliable S-readings and plots of Ts-Tp versus Tp gave unsatisfactory results with a wide scatter of Vp/Vs values.

We plotted Wadati diagrams for the best recorded local events using all weighted S-travel times (Figure 18a) and for a limited number of events using only S-travel times from horizontal components (Figure 18b). A linear least squares fit was made for each plot and the Vp/Vs ratios and Poisson's ratios were calculated. Confidence intervals of 90, 95, and 99 percent for Vp/Vs were also determined (Graybill, 1976). Table 6 is a summary of the results. Figure 18a plotted using S-phases weighted 3 or better for 37 of the well recorded local events gives a Vp/Vs ratio of 1.52 + 0.09 and Poisson's ratio of 0.11 + 0.05. The correlation coefficient is 0.95 which indicates a straight line correlation between the P- and S- travel times. To check the reliability of the Vp/Vs value of 1.52 which is quite low compared with the global average of 1.78, we plotted data from only the horizontal components to check for systematic errors introduced in reading S- arrival times from vertical components which would lower the value of Vp/Vs (Figure 18b). The Vp/Vs value using the horizontal components is 1.53 + 0.12 and the Poisson's ratio 0.13 + 0.06. The correlation coefficient is 0.96 and indicates a good linear relationship between P- and S-. Figures 18a and b demonstrate that the arrival times of S-phases picked using the vertical geophones are within the error limits of the S- picks from the horizontal geophones.

Regional events. Vp/Vs ratios for the regional events were derived using Wadati's method for four of the best recorded regional events. Figures 19a-d

TABLE 6. Vp/Vs ratios and Poisson's ratios in the Sao Miguel region

Area	Vp/Vs (b)	Correlation Coefficient	Poisson's Ratio ( )	Coefficient k for computing confidence limits* 90%	95%	99%
Agua de Pau**	1.52	0.963	0.11	0.09	0.11	0.14
Agua de Pau***	1.53	0.963	0.13	0.12	0.14	0.20
Regional events	1.62	0.984	0.19	0.05	0.07	0.09

* Confidence limits are b + k

** Data from vertical and horizontal geophones for 35 local events

*** Data from only horizontal geophones for 27 local events

show Wadati diagrams for four selected events. The resulting Vp/Vs ratios show a wide scatter and are in the range of 0.91-1.98 reflecting the poor resolution resulting from using a limited number of data points for each event. To find an average Vp/Vs value for the regional events we plotted the phase data from the nine regional events on a modified Wadati plot with only weighted arrivals of 3 or better (Figure 19e). The resulting best fit line for the regional events gives a value for Vp/Vs of 1.62 + 0.05 and Poisson's ratio 0.19 + 0.02. The correlation coefficient for the data is 0.98. The data for the regional events is summarized in Table 6. Figure 19f is a bar graph showing the error limits of Vp/Vs for two local event data sets and on regional event data set.

There are two key observations that can be made on our Vp/Vs measurements: (1) the difference between Vp/Vs values computed using local and regional events (about 7 percent); and (2) the generally low Vp/Vs value for both regional and local event data sets, compared with the global average value of 1.78. We are unable to assign a high level of confidence for the difference between Vp/Vs for local and regional events as can be seen from the bar graph (Figure 19f). However, the difference if real is not surprising as the local events represent Vp/Vs in a crustal volume of complex volcanic rock around the Agua de Pao volcano, whereas the Vp/Vs value using regional events are for sub-moho ray paths associated with the Pn and Sn phases of the regional events. One would expect the regional Vp/Vs value to correspond to that for fairly homogeneous basaltic upper mantle. This is not the case as the Vp/Vs value for basaltic samples from the Atlantic Ocean measured in the laboratory is about 1.86 (Christensen and Salisbury, 1972).

A plausible explanation for the low Vp/Vs value in the crust beneath Agua

de Pao can be given in terms of the presence of a fractured geothermal reservoir in which the temperatures are close to that at water-steam transition. We are unable to explain the cause for the abnormally low regional Vp/Vs values beneath Isla Sao Miguel. Presence of partial melt is not an acceptable explanation as melt inclusions tend to reduce S-wave velocity resulting in a higher than normal Vp/Vs ratio. Mineralogical differences from the surrounding region (Kern and Richter, 1981), presence of fractures filled with water at temperature near that needed for transition to steam, or erroneous identification of the S-phases are possible explanations. The S-phases for several of the regional events were not recorded because of pre-event memory and 20 second restraint on the record section. Perhaps the phase picked is not the S-wave, but the consistent correlation (Table 6) between events indicates we are accurately identifying the S-phase.

Residual analysis

Teleseismic P-residual and attenuation studies have been extensively used to delineate zones of anomalous seismic-wave velocities associated with magmatic heat sources in several geothermal areas in the U.S.A.(Yellowstone: Iyer et al., 1981; The Geysers-Clear Lake area: Iyer et al., 1978; Oppenheimer and Herkenfoff, 1981; Ward and Young, 1980; Long Valley-Mono Craters: Steeples and Iyer, 1976; Achauer et al., 1984; Coso Hot Springs: Reasenberg et al., 1980; Young and Ward, 1980; Roosevelt Hot Springs: Robinson and Iyer, 1981; San Francisco Mountain: Stauber, 1982; Newberry Volcano: Stauber et al., 1984; Medicine Lake Volcano: Evans, 1982). In São Miguel, due to the high ambient seismic noise level, we did not record any teleseisms and hence could not carry out a typical P-delay study. However, we were able to use the regional

vents to map P-residual patterns in the Agua de Pau area using a modified version of the teleseismic experiment. The term "P-delay" refers to the increase in travel-time as seismic P-waves traverse through a low-velocity body, such as a magma chamber. If the P-waves travel through a homogeneous, isotropic medium, the arrival times of P-phases at a series of recording instruments emplaced on the surface will reflect a constant velocity of travel and no travel-time residuals (advances or delays) are observed. On the other hand, if the waves sample an anomalous low-velocity zone such as a magma body, or a volume of denser, high-velocity medium such as a mafic intrusion, the arrival-times will give measurable travel-time residuals. Positive residuals or P-delays are associated with low-velocity bodies and negative residuals or P-advances are associated with high-velocity bodies.

To calculate residuals the P-arrival times for each of seven of the well-recorded regional events were fitted using least-squares to a plane wave-front to obtain an average apparent velocity and azimuth of travel. The P-residuals at each station were simply the deviation of the arrival time from the predicted least-squares-fitted arrival times. Note that the residuals calculated using this method are independent of the earthquake locations and origin times. The azimuths of the events were 16°, 126°, 263°, 308°, 309°, 309°, and 330°. The residuals from the three events at azimuths 303°, 306°, and 313° were averaged and these events will be treated as one event in the subsequent discussion. The apparent velocities, azimuths and residuals for all the events are shown in Table 7 and the residuals for the five azimuth groups are desplayed in Figure 20. Note that in spite of the sparse data set, residuals from all the azimuths except 263° show positive residuals or delays around the Agua de Pau volcano. Superimposed on this is a pattern of azimuthally varying residuals. To highlight the azimuthally invariant

component of the residual pattern, we have averaged all the residuals (Figure 21a). Note the east-west elongate zone of P-delays with an amplitude of 0.1 to 0.2 seconds centered on Agua de Pau volcano. In interpreting this pattern of delays, the first question to ask is whether it is related to elevation effects. The build up of low velocity debris around a volcano can produce a spatial delay pattern as has been observed. In Figure 22 we have plotted elevation versus average residuals. Note that except for FAC and CML, the two stations on the western extension of the anomaly along the center of the island, the elevation versus distance gives an approximately linear regression with a slope indicating about 0.2 sec delay for 1 km of elevation increase. Assuming an average upper-crustal layer velocity of 3.2 km/sec velocity (used in earthquake location, Table 4) means a further decrease of 40% in velocity over the region indicated by the delays. A second explanation for the delays is to assume that the linear relationship between residuals and elevation is a fortuitous result of the deeper processes of volcano building and is caused by an extended crustal low-velocity zone. Since the seismic waves used in this study are most probably Pn phases (the uncertainty is because of lack of good hypocentral locations) with an emergent angle of 45°, the observed delays could be interpreted to have been caused by a low-velocity body, elongate in an east-west direction, beneath the Agua de Pau volcano. The body could be 10 km long and 5 km wide, extending from the surface to a depth of about 5 km. The velocity decrease within the body from the surrounding rock could be about 10%. A plausible explanation for such a low-velocity body could be that it is caused by a large steam reservoir within the upper crust. The possibility for the existence of a well fractured geothermal system in the area of Agua de Pau is supported by the hydrothermal sampling and geophysical studies performed by the USGS, the surficial expressions of a geothermal system at hot springs such

as Lombadas and Caldieras, and the generally low Vp/Vs ratios discussed earlier. Such a steam reservoir can explain the low VP/Vs and low P-wave velocities inferred from the delays because steam-filled fractures in rock volumes result in lower than normal P-velocities (Ito et al., 1979). Another explanation for a crustal low-velocity body is the presence of partial melt (Iyer and Stewart, 1977). We are unable to discriminate between the proposed delay-causing mechanisms due to lack of adequate geologic and other geophysical data. Use of detailed geologic maps to relate surface lithology with the observed residuals, teleseismic studies and seismic refraction surveys (see recommendations) are needed to interpret the observed delay anomaly.

Let us now explore the first possibility that the averaged residuals reflect variations in the top layers of the crust. In order to look at variations in the P-velocities at depth (deeper than 1-2 km) we subtracted the average residuals from the residuals for each event. The resulting values should approach zero if all variations in P-wave velocities are due to structure in the top crustal layers. Figures 21b-f are plots of the residuals derived for each event with the average residuals subtracted from them. The patterns show clear evidence for azimuthal variation with two different patterns for northerly and southerly events. The results are intriguing, but the minimal number of events and their ambiguity leave interpretation open to discussion.

We now return to the residual pattern for the event from the east (Figure 21c) which did not fit into the delay pattern of the other events. A clue for the different behaviour of this event is provided by the similarity between the residual pattern without and with the average residuals subtracted (20b and 21c). In both cases instead of delays, P-advances are found around the

Agua de Pau volcano. If the event is farther away from the seismic array than the other regional events resulting in deeper penetration of the seismic waves into the mantle, the P-advances can be interpreted as due to anomalous high-velocity upper mantle beneath the central part of Sao Miguel. The effect of the upper mantle anomaly could be more predominant than the surface effect on the residuals and could explain the residual pattern with no correction. However, this inference is very tentative an needs more well-constrained data to support it.

We have used the average station delay terms derived from the plane wave residuals of the regional events in locating the regional and local earthquakes using the HYPO71 program. The routine gives station residuals for the regional events which can be plotted similarly to the plane wave residuals. Near surface structure is eliminated with the station terms and so the residuals should reflect structure at depth. Residuals given by HYPO71 are derived by subtracting the calculated P-wave travel time and station delay from the observed P-wave travel time. Figure 23 is a plot of the average station residuals for the regional events using the HYPO71 program and probably reflects deeper structure beneath the Agua de Pau volcano.

Discussion

The signficant finding of this study is that the seismic activity recorded during this experiment was not centered under the Agua de Pau massif or associated with any known geothermal manifestations such as Lombadas or Caldeiras. Instead, the seismic activity was centered on the east slope of Agua de Pau extending into the topographic low between the Agua de Pau and Furnas volcanoes. It must be noted that only the larger events (M>1.5) which

occurred within the network triggered 50 per cent or more of the portable stations. Station VIF triggered the three institute recorders so there is a bias toward events occuring in the vicinity of station VIF. Few events occurred to the south of station VIF indicating the activity recorded to the north of the station is a true sample of seismic activity in the vicinity of Agua de Pau. The seismic activity we observed is by no means a true sample of the total activity for the island of São Miguel. We had no stations on either the west end of the island near the Cete Cidades volcano, or on the east end of the island near the Furnas and Povoacoa volcanic centers. The active geothermal system including hot springs at Furnas suggests that micro-earthquake activity could be present in that area. It is estimated that events less than M_D 2 which occurred 15 km from the center of our network would not be sensed by the required 3 or more stations for proper locating purposes. Thus, if activity is present at the Cete Cidades and Furnas volcanoes, it is of the order of that about Agua de Pau, or perhaps less. Also, the large number of seismic triggers which could not be located indicates that the seismicity of São Miguel is probably much higher than that implied by the small number of events located in this study.

There are several explanations for the location of the activity to the east of Agua de Pau. First, the activity could be associated with the geothermal system described by Muffler and Duffield (1984), although no surface manifestations of the geothermal zone are visible in the area of seismic activity. Fumaroles and hot springs such as Lombadas and Caldeiras occur in deeply eroded canyons on Agua de Pau and since the east side of Agua de Pau is not deeply eroded, the geothermal system may well be masked by the overlying deposits. Secondly, the activity could be a result of regional stress release along the Terceira rift. The structure of the rift zone is not

well defined on the east side of Agua de Pau because of recent volcanic deposits which cover most structure and faults. We attempted to derive focal mechanisms for the larger local events but the first motions showed compressional motions across the whole array. Since all the stations are closely spaced over the area of activity we see only the upper hemisphere in the focal solution and the results are expected. Finally, many of the studies concerning Sao Miguel indicate a large rhyolitic magma chamber underlies the central and eastern portion of Sao Miguel (Booth et al., 1978, Muffler and Duffield, 1984, Gandido, 1964). The seismic activity could be associated with minor inflation or deflation of the postulated magma chamber. No tilt or detailed deformation studies have been done to substantiate this theory and our seismic study does not give definitive evidence for a large magmatic anomoly under central São Miguel.

All of the studies done by the USGS indicate an active geothermal system exists under the upper portion of Agua de Pau, with the most likely prospects on the north and east sides of the volcano. The low Vp/Vs ratio of 1.52 for local earthquakes in this area and the P-delays in the same locality suggest the presence of a steam reservoir under the Agua de Pau volcano extending 3 to 5 km to the east of the summit. Senos and Nunes (1976) cite evidence of a zone of attenuation under the Furnas volcano and low (1.56) Vp/Vs values in that area. Combining the evidence from our data with his indicates that there is a zone of attenuation, most likely a steam reservoir, beneath the entire central and eastern portion of São Miguel.

Earthquake and Volcanic Hazards. It must be stressed that the seismic activity present in the Agua de Pau volcano region is an ongoing process. The possibility of large magnitude events is low, but can not be discounted. The

January 1, 1980 M 7.2 event that destroyed many buildings on Isla Treceira is an example of the type of event that could occur. however, the short duration of our seismic study does not permit any defenitive conclusions on the possibility of occurrence of a destructive earthquake in São Miguel in the future.

The youthful calderas and recent volcanic activity at all of the volcanic centers on Sao Miguel, as well as the documented ages of eruptions by Booth et al., (1978) show that future eruptions should be expected . The documented eruptive histories of the volcanoes on São Miguel average an eruption cycle of about every 500 years for a magnitude 6 eruption and every 200 years for a magnitude 5 eruption. The occurrence of two swarms of seismic activity in a three month period seems suspiciously related to the Agua de Pau and Furnas volcanoes, though again no clear diagnostics are available as to the volcanic nature of the seismic activity. Seismic monitoring of the microearthquake activity on Sao Miguel must be upgraded so that an accurate record of activity can be built for future reference. Deviations from the normal pattern of seismicity should be noted so that the possibility of an impending eruption can be prepared for.

Magma Chamber. One of the purposes of our study was to detect any magma chamber present within the Agua de Pau volcano. The residuals obtained from the regional events do not definitively define a magma chamber, even though as discussed earlier they could be interpreted as due to a crustal low-velocity body in which the P-wave velocity is lower than normal by about 10%. The body could be a result of a dry-steam reservoir or a partially molten magma chamber beneath Agua de Pau. There is also marginal evidence for a high-velocity

intrusion in the upper mantle. Our data are inconclusive and need to be supported with further detailed seismic surveys to verify the suggestive patterns that we see. The low Vp/Vs ratios of local events can be attributed to slow surficial deposits, but could also be due to a steam charged geothermal system.. If the existence of a large steam reservoir beneath the central and eastern portion of São Miguel is accepted, then the magmatic system that drives the system must be accounted for. Booth et al. (1978) have shown that between about 5000 and 7000 years before present there were at least 13 basaltic eruptions around the flanks of Agua de Pau and Furnas. During the past 5000 years there have been no basaltic flank eruptions in the same area. They suggest that a lateral spreading of the trachytic magma chamber that supplies Agua de Pau occured at about the time of the Fogo A eruption (4550 years b.p.). The subsequent reduction of basaltic flank eruptions may be a result of the inability of the basaltic magma to penetrate the trachytic magma. Lagoa do Congro and Logoa de S. Braz occupy craters between Agua de Pau and Furnas, both are post Fogo A trachytic eruption centers indicating a trachytic magma chamber or feeder system exists under the central and eastern area of Sao Miguel. It should be noted that basaltic eruptions continued during the past 5000 years with at least 37 events occuring during this period, all to the west of Agua de Pau with none in the major calderas. In conclusion, the presence of a large trachytic magma chamber beneath Agua de Pau and perhaps the entire central and eastern section of Sao Miguel has been postulated by several authors. Our study shows no large magmatic anomaly appears to exist under Agua de Pau at least in the top five kilometers, although Vp/Vs ratios and P-delays in the area certainly suggest the presence of some type of anomaly.

Recommendations

The presence of seismic activity, higher than we expected, leads us to recommend several studies which would help to better understand the active geothermal, seismic, and volcanic processes occuring on Sao Miguel.

(1). The first and most important recommendation is to upgrade the existing monitoring network. The paper recorders now used do not have the sensitivity to detect small magnitude microearthquakes. An island-wide network that would enable the detection and location of events to the M 1 level would greatly improve the understanding of seismic activity on the island. Because of the high level of noise on the island we recommend that the present stations and any future stations be installed in boreholes to reduce the problem of surficial noise and to enhance the detection capabilities of the network. Such a network should provide, (a) a background seismicity level against which to monitor seismicity changes associated with future geothermal development, (b) seismic monitoring for detecting pre-cursory seismic activity preceding hazardous volcanic eruptions, and (c) seismicity studies for earthquake prediction and earthquake hazard evaluation. It is also recommended that a state-of-the-art computer oriented seismic data analysis center be set up to process the data from the seismic array.

(2). The effectiveness of a seismic network depends on how precisely earthquake hypocenters can be determined. For all the studies mentioned abo ve, earthquake location accuracy to a fraction of a kilometer in hypocenter and depth is required. The critical data to achieve such a precision beside accurate P- and S-arrival times over a dense seismic network, are detailed velocity models from seismic refraction/reflection experiments.

The available refraction data in São Miguel (Senos and Nunes, 1976) is inadequate and so we propose a comprehensive refraction/reflection experiment. Instruments, field procedures, and analysis techniques for such an experiment are highly developed in many institutions of the world and particularly in the U.S. Geological Survey (Healy et al., 1982; Zucca et al., 1982; and Fuis et al., 1984). The small dimensions of Isla São Miguel (60 km x 15 km) would permit deployment of dense profiles of portable seismic stations on the island and detonation of large shots in the ocean to evolve detailed velocity models.

(3). An extension of the Seismic refraction study is a seismic imaging experiment to model in three dimensions lateral and vertical velocity heterogeneities associated with the geothermal and volcanic system in the Agua de Pau-Furnas area of Sao Miguel. The experiment consists of deploying a two-dimensional array of about 100 instruments in a 10 km x 10 km area with average instrument spacing of about 1 km, and setting off large shots (in the ocean) around the array (Stauber, 1984). The travel-time residuals from the vertically arriving Pg, Pn and reflected phases can be inverted to produce a comprehensive image of the seismic velocity anomalies.

(4). We strongly recommend a teleseismic P-residual study of the whole of Sao Miguel, The strategy would be to supplement the proposed seismic network with several portable stations to achieve an average instrument spacing of about 5 km and collect teleseismic and regional event data for several months. The analysis of data from such a study would provide a 3-dimensional model of the crust and mantle beneath Sao Miguel with a resolution of about 5 km. This model would complement the high-resolution model from the seismic imaging experiment proposed under (3). Also, the experiment can be expected to provide a wealth of data to explore in detail the seismicity, Vp/Vs, and residual anomalies discussed earlier in this report. The excellent data set

thus collected can be used for numerous studies related to the seismicity, tectonics, volcanology, and geothermal potential of São Miguel.

REFERENCES

Aki, K., 1982, Three-dimensional seismic inhomogeneities in the lithosphere and asthenosphere: evidence for decoupling in the lithosphere and flow in the asthenosphere, Reviews of Geophysics and Space Physics, 20, 161-170.

Assuncao, C. F. T. de, 1961, Estudo petrografico da ilha de S. Miguel (Acores), Com. Serv. Geol. Portugal, 45, 61-176.

Bakun, W. H., 1984, Seismic moments, local magnitudes, and code-duration magnitudes for earthquakes in central California, Bull. Seism. Soc. Am., 74, 439-458.

Booth, B., Croasdale, R., and Walker, G. P. L., 1978, A quantitative study of five thousand years of volcanism on Sao Miguel, Azores, Philos. Trans. R. Soc. London, 288, 271-319.

Castello Branco, A. de C., Zbyszewski, G., Medeiros, A. C. de, and Almeida, F. M. de, 1957, Etude geologique de la region de Furnas dans l'Ile de S. Miguel (Acores), Com. Serv. Geol. Portugal, 38, 5-64.

Chaterjee, S. N., Pitt, A. M., and Iyer, H. M., 1984, Vp/Vs ratios in the Yellowstone National Park region, Wyoming, J. of Volcan. and geotherm. Res. (in press).

Duffield, W. A., and Muffler, L. J. P., 1984, Geothermal Resources of Sao Miguel, Azores, A summary report for USAID.

Eberhart-Phillips, D., and Oppenheimer, D. H., 1984, Induced seismicity in the Geysers geothermal area, California, J. Geophys. Res., 89, 1191-1207.

Evans, J. R., 1982, J. Geophys. Res., 87, 2654-2670.

Feraud, G., Kaneoka, I., and Allegre, C. J., 1980, K/Ar ages and stress pattern in the Azores: geodynamic implications, Earth and Planetary Science Letters, 46, 275-286.

Fuis, G. S., Mooney, W. D., Healy, J. H., McMechan, G. A., and Lutter, W. J., 1984, A seismic refraction survey of the Imperial Valley Valley Region, California, Journal of Geophys. Res., 89, 1165-1189.

Gandido, A., Guidi, M., Merlo, C., Mete, L., Rossi, R., Sommaruga, C., and Zan, L., 1984, Preliminary model of the Ribeira Grande geothermal field (Azores Islands), United Nations Economic Commission for Europe Seminar on Utilization of Geothermal Energy for Electric Power Production and Space Heating, Florence, Italy.

Geonomics, 1977, Microearthquake seismology survey, Task IV, of the Sao Miguel geothermal project, submitted to IGA, Azores.

Graybill, F. A., 1976, Theory and application of the linear model, Duxbury Press.

Healy, J. H., Rubey, W. W., Griggs, D. T., and Raleigh, C. B., 1968, The Denver earthquakes, Science, 161, 1301-1310.

Healy, J. H., Mooney, W. D., Blank, H. R., Gettings, M. E., Kohler, W. M., Lamson, R. J., and Leone, L. E., 1982, Saudi Arabian seismic deep-refraction profile: final project report: U.S Geological Survey Saudi Arabian Mission and Directorate General of Mineral Resources, Open-File Report USGS-OF-02-37, 432pp.

Hirn, A., Haessler, H., Hoang-Trong, P., Wittlinger, G., Mendes Victor, L. A., 1980, Aftershock sequence of the January 1st, 1980, earthquake and present-day tectonics in the Azores, Geophyisical Research Letters, 7, 501-504.

Ito, H., DeVilbiss, J., and Nur, A., 1979, Compressional and shear waves in saturated rock during water-steam transition, J. Geophys. Res., 84, 4731-4735.

Iyer, H. M., 1984, Geophysical evidence for the locations, shapes and sizes, and internal structures of Magma chambers beneath regions of Quaternary volcanism, Phil. Trans. R. Soc. Lond., A 310, 473-510.

Iyer, H. M., Evans, J. R., Zandt, G., Stewart, R. M., Coakley, J. M., and Roloff, J. N., 1981, A deep low-velocity body under the Yellowstone caldera, Wyoming: delineation using teleseismic P-wave residuals and tectonic interpretation, Geol. Soc. Am. Bull., 92, Part I: 792-798, Part II (Microfiche edition): 1471-1646.

Iyer, H. M., Oppenheimer, D. H., and Hitchcock, T., 1979, Abnormal P wave delays in the Geysers-Clear Lake geothermal area, California, Science, 204,
495-497.

Iyer, H. M., and Stewart, R. M., 1977, Teleseismic technique to locate magma in the crust and upper mantle, in Proceedings of the American Geophysical Union Chapman Conference on Partial Melting in the Earth's Upper Mantle: H. J. B. Dick, Editor, Bulletin 96, 281-299, Oregon Department of Geology and Mineral Industries, Portland Oregon.

Jeremine, E., 1957, Etude microscopique des roches de la region de Furnas (S. Miguel, Acores), Com. Serv. Geol. Portugal, 38, 65-90.

Kern, H., and Richter, A., 1981, Temperature derivatives of compressional and shear wave velocities in crustal and mantle rocks at 6 kbar confining pressure, J. Geophys., 49, 47-56.

Kissling, E., Ellsworth, W. L., and Cockerham, R. S., 1984, Three-dimensional structure of the Long Valley Caldera, California, region by geothomography, J. Geophys. Res. (in press).

Kissingler, C., and Engdaho, E. R., 1973, The interpretation of Wadati diagram with relaxed assumptions, Bull. Seis. Soc Am., 63, 1723-1736.

Klein, F. W., Einarsson, P., and Wyss, M., 1977, The Reykjanes Peninsula, Iceland, earthquake swarm of September 1972 and its tectonic significance, J. Geophys. Res., 82, 865-888.

Krause, D. C., and Watkins, N. D., 1970, North Atlantic crustal genesis in the vicinity of the Azores, Geophys. J. R. astr. Soc., 19, 261-283.

Laughton, A. S., Whitmarsh, R. B., Rusby, J. S. M., Somers, M. L., Revie, J., McCartney, B. S., and Nafe, J. E., 1972, A continuous east-west fault on the Azores-Gibraltar ridge, Nature, 237, 217-220.

Lee, W. H. K., Bennett, R. E., and Meagher, K. L., 1972, A method of estimating magnitude of local earthquakes from signal duration, U.S. Geol. Surv. Open File Report, 37 p.

Lee, W. H. K., and Lahr, J. C., 1975, HYPO71 (Revised); A computer program for determining hypocenter, magnitude and first motion pattern of local earthquakes, Open File Rep. 75-311, U.S. Geol. Surv., Menlo Park, California

Machado, F., 1966, Anomalias das Intensidades do Terramoto de S. Miguel, Acores em 1522, Boletin do Museu e Laboratorio Mineralogico e Geologico da Faculdade de Ciencias, 10, 109-117.

Machado, F., 1973, Periodicidade sismica nos Acores, Ministerio da Industria e Technologia, Direccao-Geral dos Servicos Electricos, Direccao Geral dos Combustiveis, Comissao para o Estudo de Geotermia dos Acores-S. Miguel, Documentacao.

Machado, F., and Forjaz, V. H., 1965, A crise sismica de S. Jorge, de Fevereiro de 1964, Bol. Soc. Geol. Port., 16, 19-36.

Marks, S. M., Ludwin, R. S., Louie, K. B., and Bufe, C. G., 1978, Seismic monitoring at the Geysers geothermal field, California, Open File Rep. 78-798, U. S. Geol. Surv., Menlo Park, California.

Muecke, G. K., Ade-Hall, J. M., Aumento, F., MacDonald, A., Reynolds, P. H., Hyndman, R. D., Quintino, J., Opdyke, N., and Lowrie, W., 1974, Deep drilling in an active geothermal area in the Azores, Nature, Lond., 252 281-285.

Pichon, X. Le, Houtz, R. E., Drake, C. L., and Nafe, J. E., 1965, Crustal structure of the mid-ocean ridges, 1. seismic refraction measurements, J. Geophys. Res., 70, 319-339.

Raleigh, C. B., Healy, J. D., and Bredehoeft, J. D., 1976, An experiment in earthquake control at Rangely, Colorado, Science, 191, 1230-1237.

Reasonberg, P., Ellsworth, W. L., and Walter, A., 1980, Teleseismic evidence for a low-velocity body under the Coso geothermal area, J. Geophys. Res., 85, 2471-2483.

Richter, C. F., 1935, An instrumental earthquake magnitude scale, Bull. Seism. Soc. Am., 25, 1-32.

Robinson, R., and Iyer, H. M., 1981, Delineation of a low-velocity body under the Roosevelt Hot Spreings geothermal area, Utah, using teleseismic P wave data, Geophysics, 46, 1456-1466.

Sanders, C. O., and Ryall, F., 1983, Geometry of magma bodies beneath Long Valley, California determined from anomalous earthquake signals, Geophysical Research Letters, 10, 690-692.

Schilling, J. G., 1975, Azores mantle blob: rare-earth evidence, Earth and Planetary Science Letters, 25, 103-115.

Searle, R. C., 1976, Lithospheric structure of the Azores Plateau from Rayleigh-wave Dispersion, Geophys. J. R. astr. Soc., 44, 527-546.

Searle, R. C., 1980, Tectonic pattern of the Azores spreading centre and triple junction, Earth and Planetary Science Letters, 51, 415-534.

Senos, M. L. Conde, and Nunes, J. A. F. Costa, 1976, Report of seismic refraction on Isla Sao Miguel, Servico Meteorologica Nacional, Lisboa.

Steeples, D. W., and Iyer, H. M., 1976, J. Geophys. Res., 81, 849-860

Van Padang, M. Neumann, Richards, A. F., Machado, F., Bravo, T., Baker, P. E., and Le Maitre, R. W., 1967, Atlantic Ocean, Inter. Volcan. Assoc., Catalogue of active volcanoes-Pt 21.

Walker, G. P. L., and Croasdale, R., 1971, Two plinian-type eruptions in the Azores, J. Geol. Soc. London, 127, 17-55.

Wadati, K., 1933, On travel time of earthquake waves, Part II, Geophys. Mag., 7, 101-111.

Ward, P. L., 1972, Microearthquakes: prospecting tool and possible hazard in the development of geothermal resources, Geothermics, 1, 3-12.

Ward, P. L., and Bjornsson, S., 1971, Microearthquakes, swarms, and the geothermal areas of Iceland, J. Geophys. Res., 76, 3953-3982.

Ward, P. L., and Jacob, K. H., 1971, A study of microearthquakes and ground noise in the Ahuachapan geothermal field, El Salvador, Central America, Final Report to the United Nations Resources and Transport Division, Energy Section.

Weaver, C. S., and Hill, D. P., 1978/79, Earthquake swarms and local crustal spreading along major strike-slip faults in California, Pageoph, 117, 51-64.

Weston, F. S., 1964, List of recorded volcanic eruptions in the Azores with brief reports, Bol. Mus. Lab. Miner. Geol. Fac. Ciencas Lisboa, 10, 3-18.

Wilson, J. T., 1963, Evidence from islands on the spreading of ocean floors, Nature, 197, 536-538.

Young, C. and Ward, R. W., 1980, J. Geophys. Res., 85, 5227-5236.

Zbyszewski, G., 1961, Etude geologique de l'Ile de S. Miguel (Acores), Com. Serv. Geol. Portugal, 45, 5-79.

Zucca, J. J., Hill, D. P., and Kovach, R. L., 1982, Crustal structure of Mauna Loa Volcano, Hawaii, from seismic refraction and gravity data, Bull. Seis. Soc. Am., 72, 1535-1550.

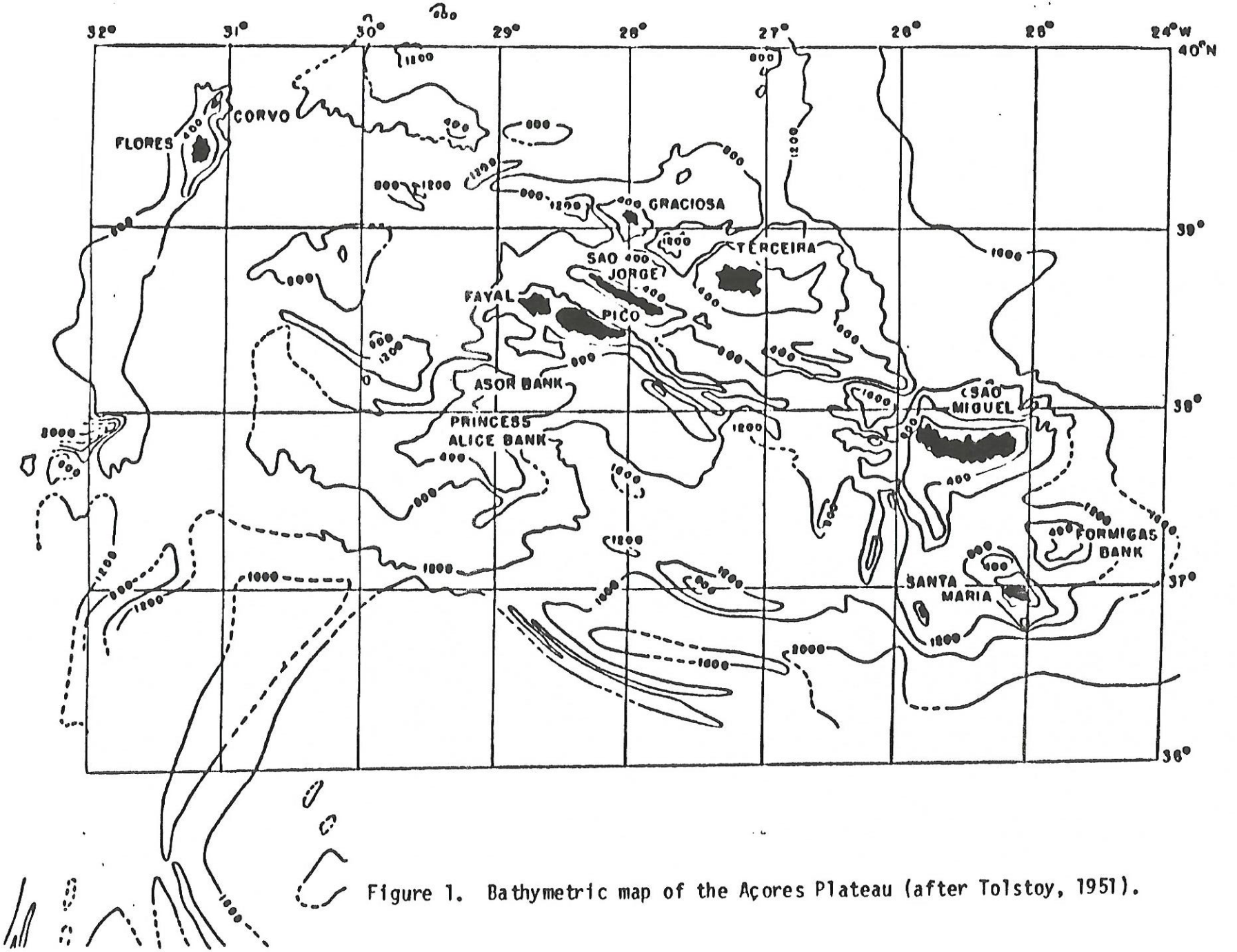

Figure 1. Bathymetric map of the Açores Plateau (after Tolstoy, 1951).

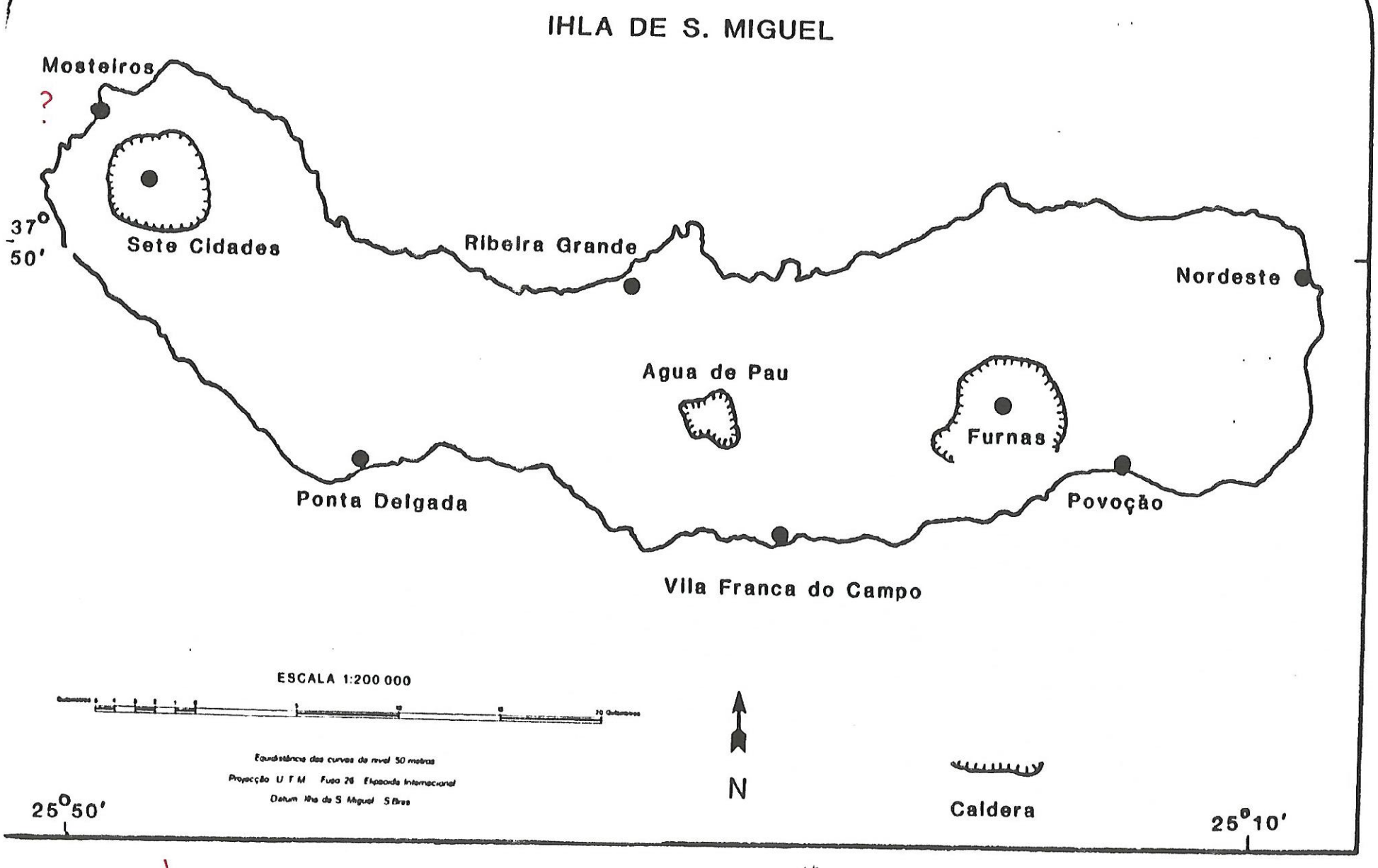

Figure 2. Sao Miguel and the volcanic centers Sete Cidades, Agua de Pau, and Furnas.

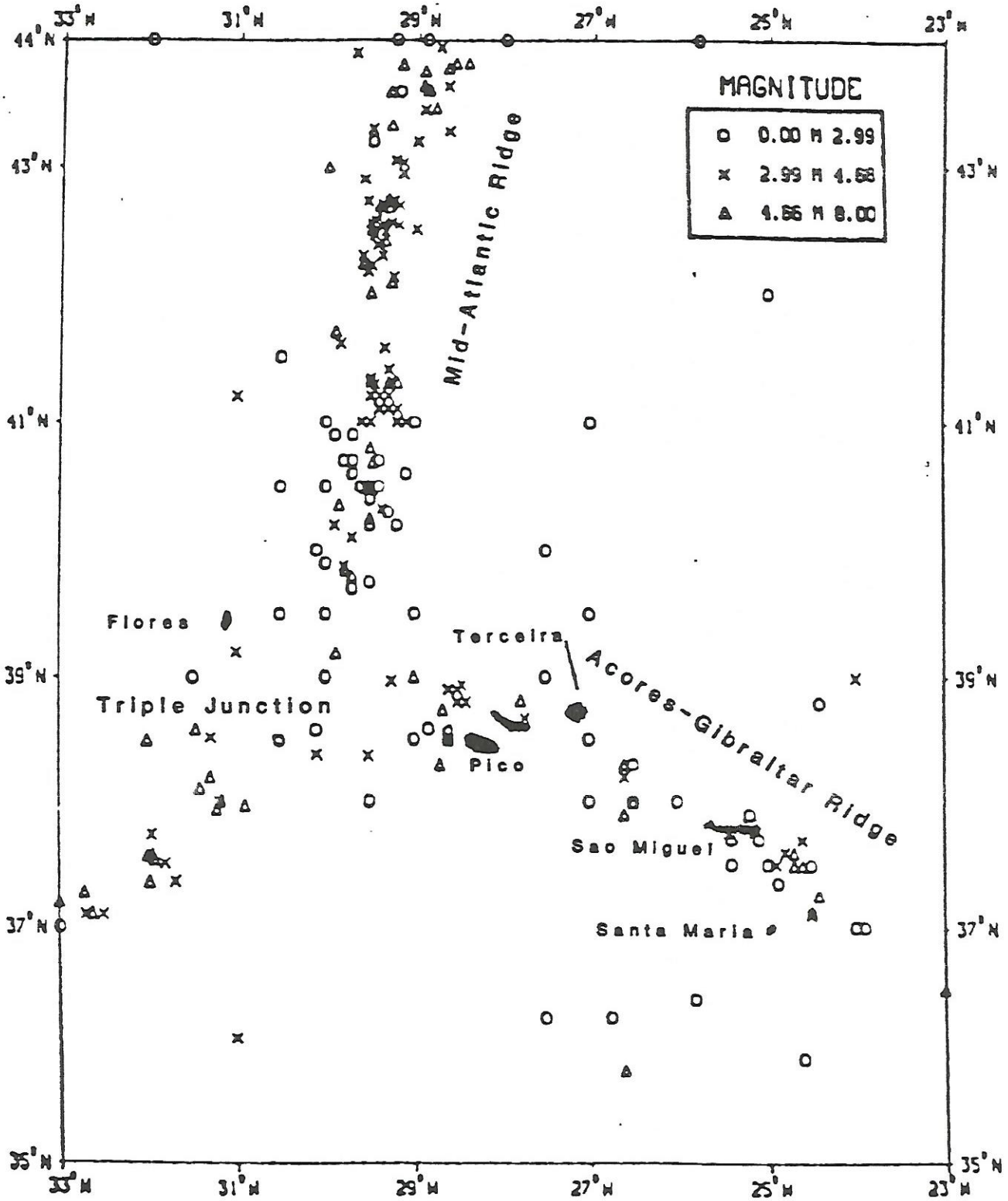

Figure 3. Regional seismicity of the Acores Plateau and Mid-Atlantic Ridge, 1970-1980. (Courtesy of National Geophysical and Solar-Terrestrial Data Center, NOAA, Boulder, Colorado).

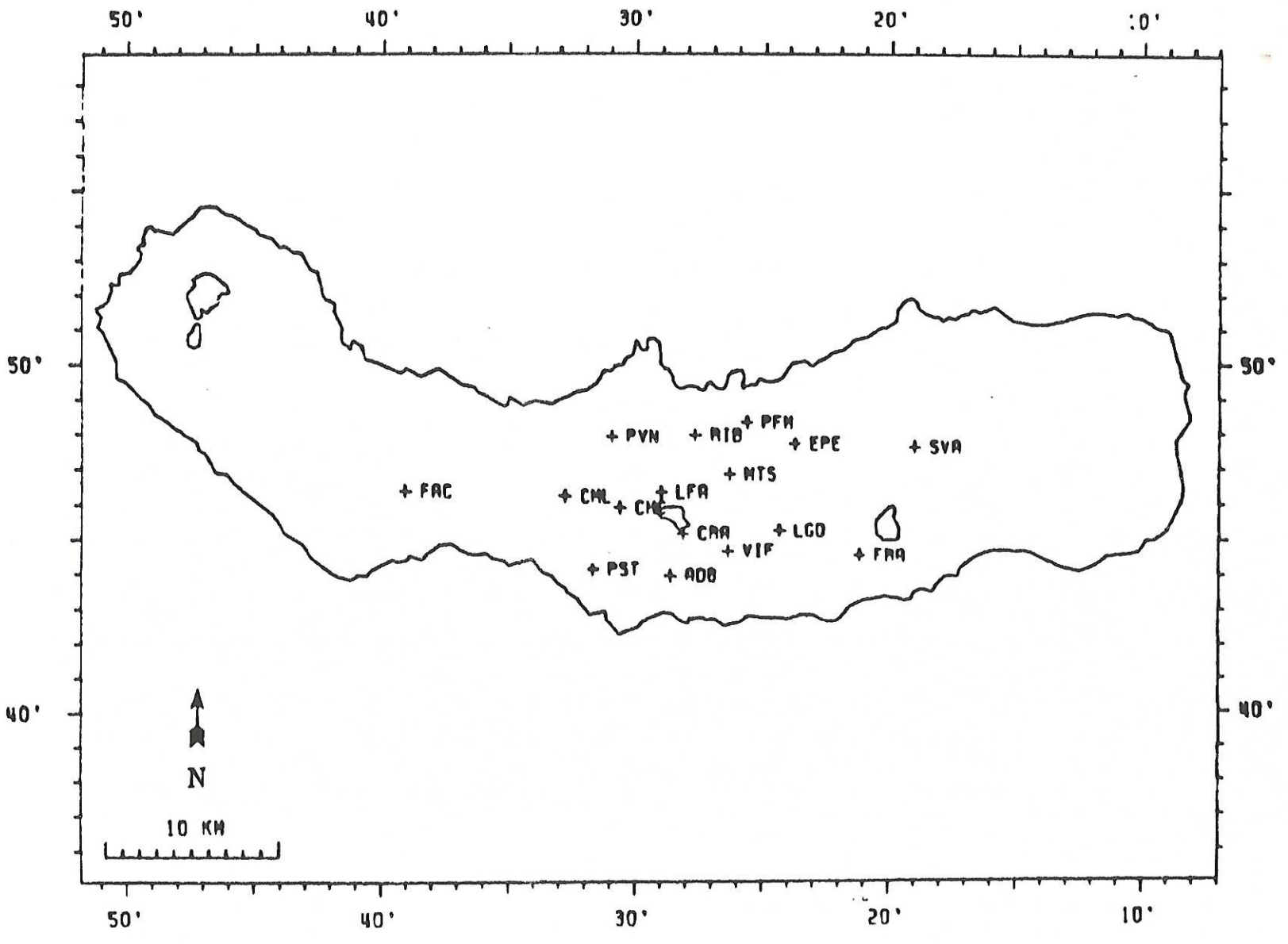

Figure 4. Station codes and locations.

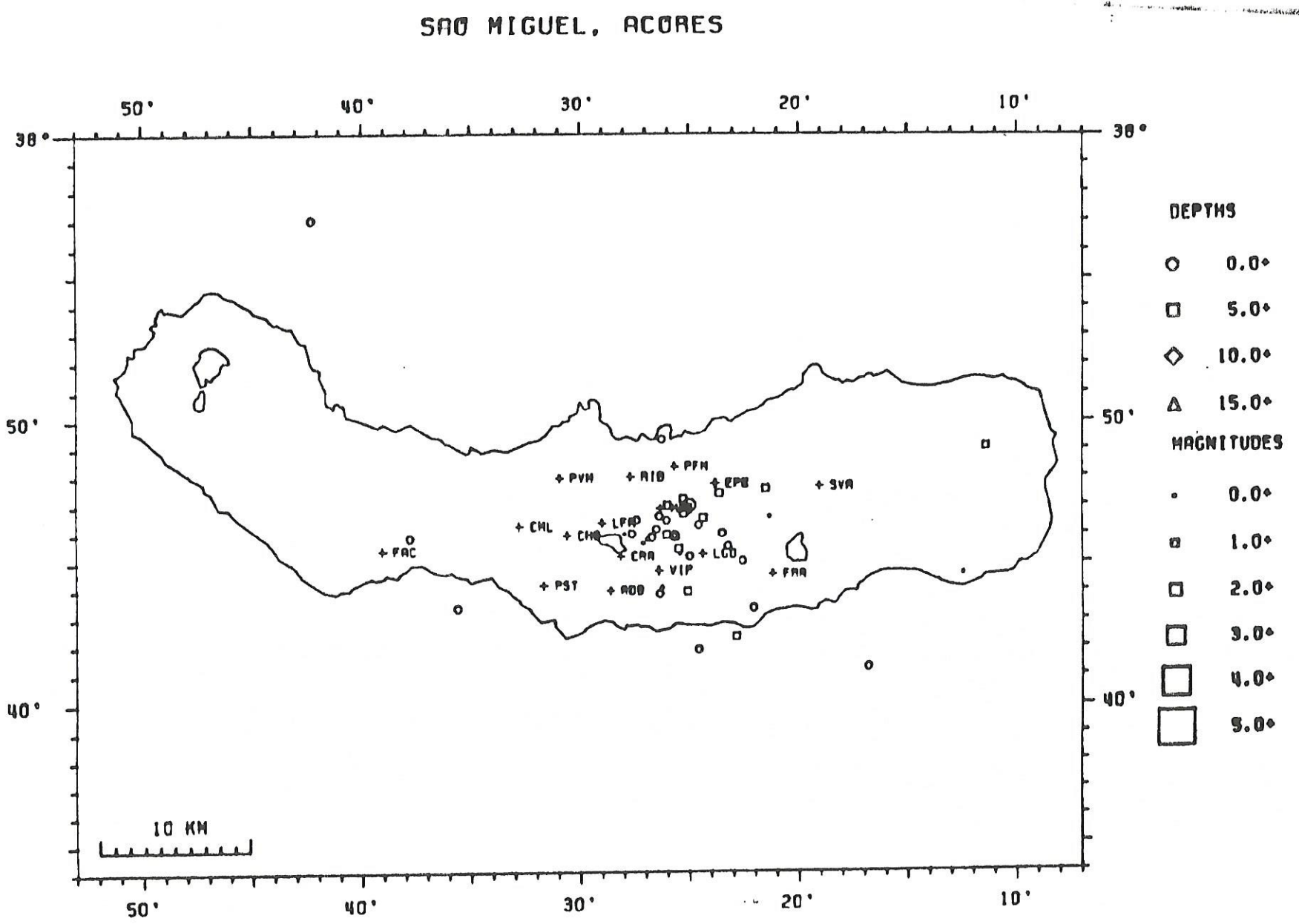

Figure 7. Spatial plot of epicenters using the initial crustal velocity model of Le Pichon (1965).

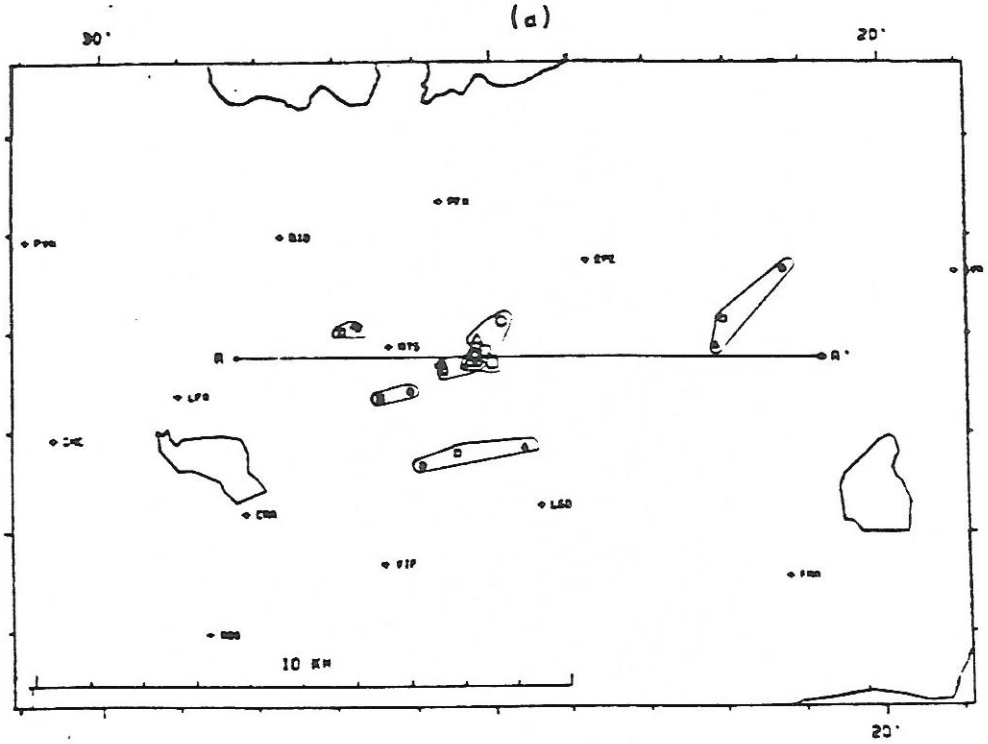

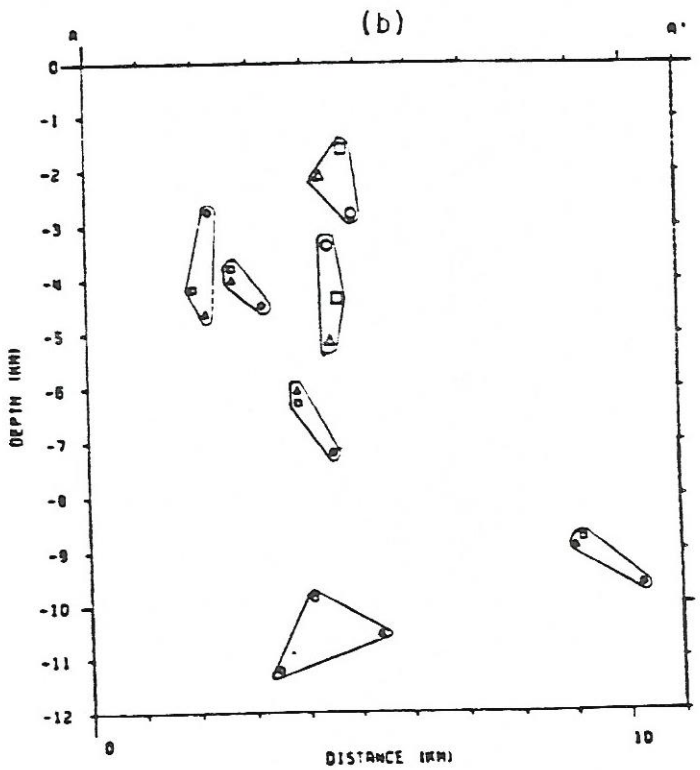

○ Three layer model from Le Pichon (1965)

□ Model from refraction data (Senos and Costa Nunes, 1976)

△ VELEST model

Figure 8. Variation in epicentral locations using three different crustal velocity models; (a) map view, and (b) depth cross-section along A-A'.

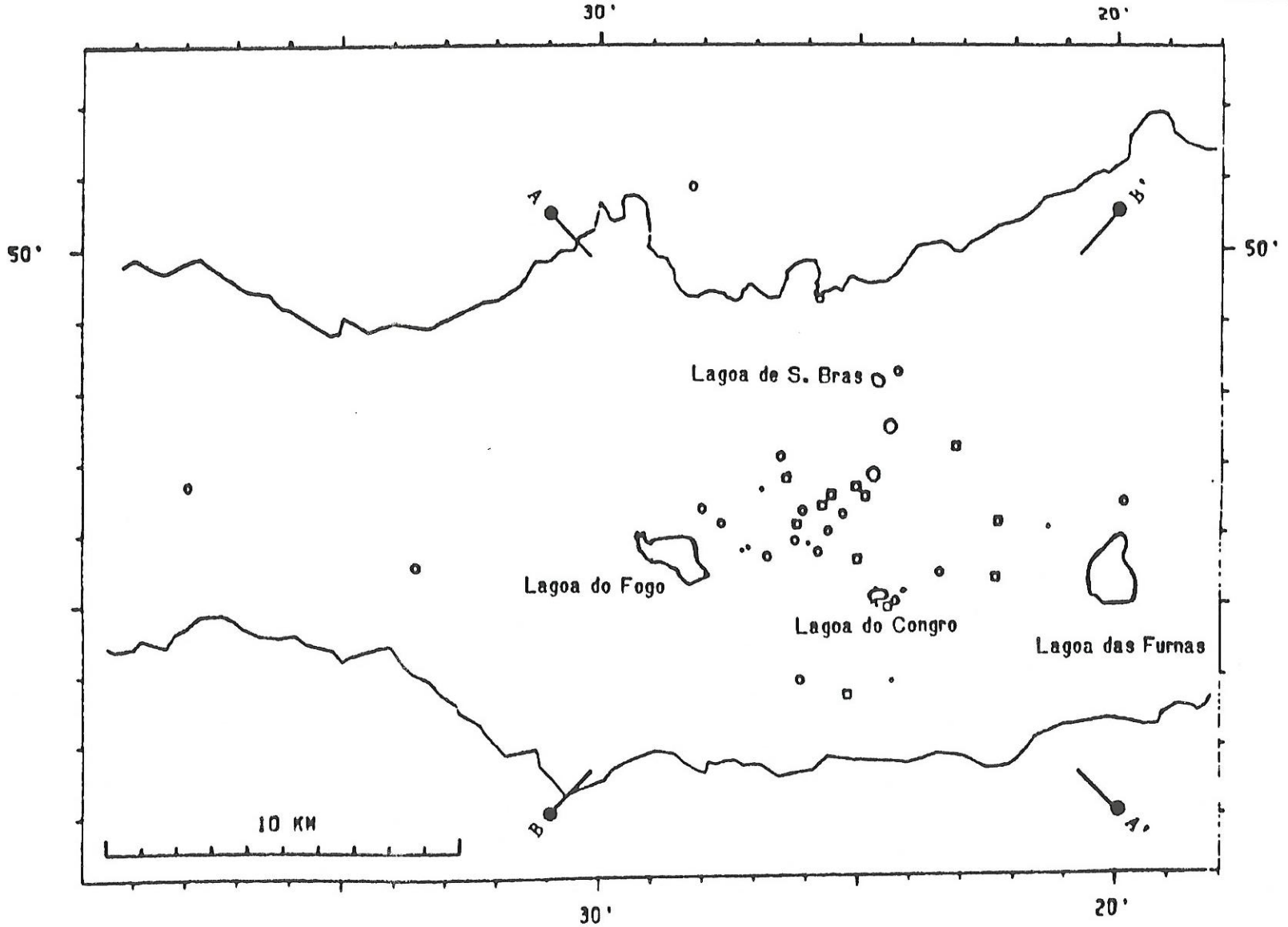

Figure 9. Spatial plot of earthquake epicenters in central Sao Miguel, June 16, 1983 to October 10, 1983. The events were located with the VELEST crustal model, and station terms derived from the regional earthquake residual analysis.

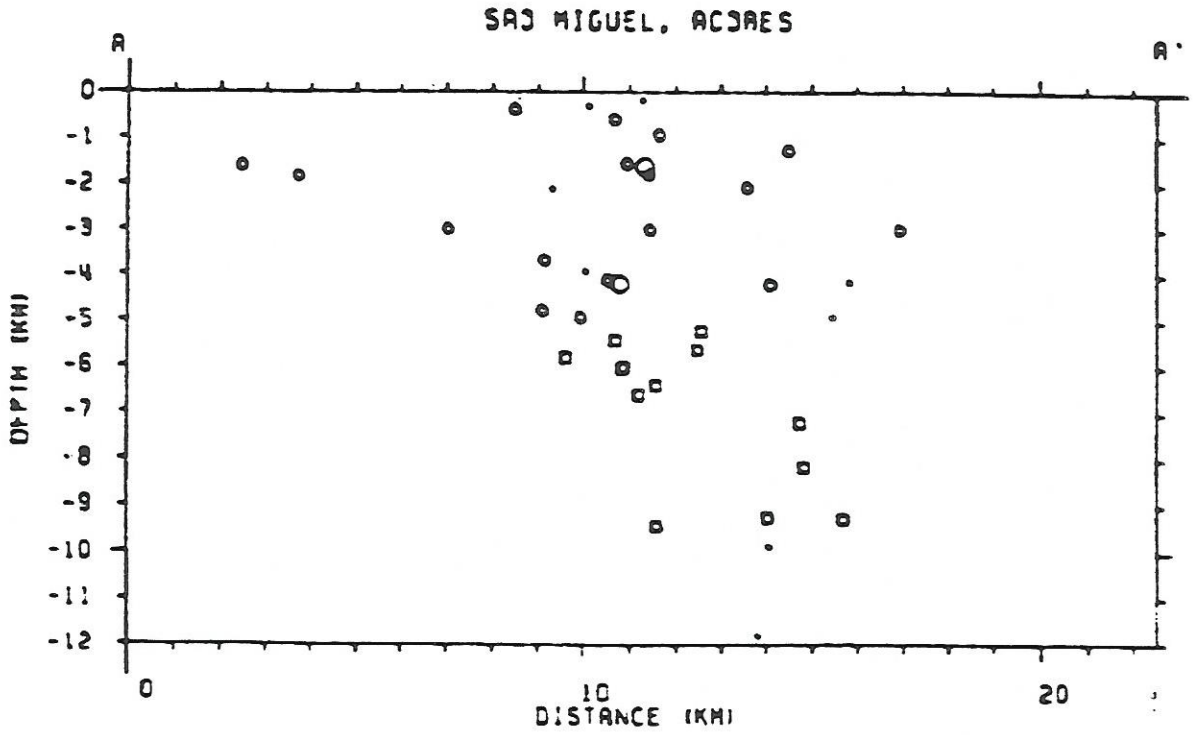

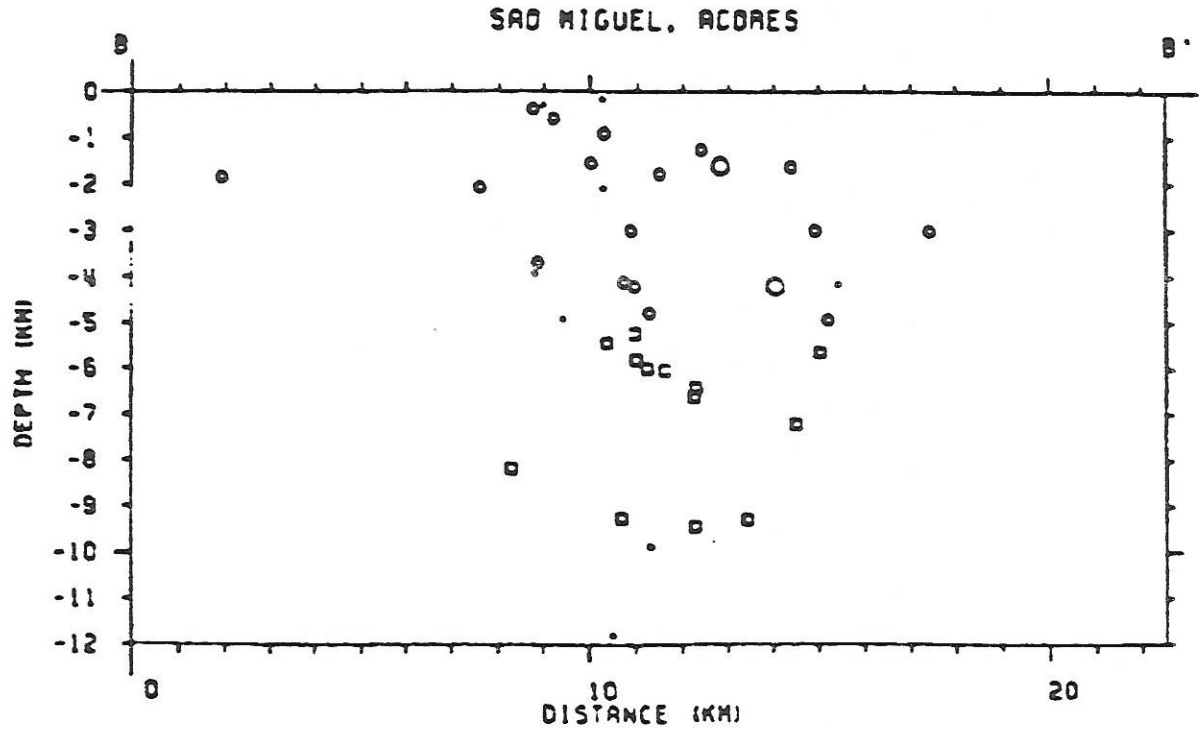

Figure 10. Depth cross-sections along A-A' and B-B' from Figure 9.

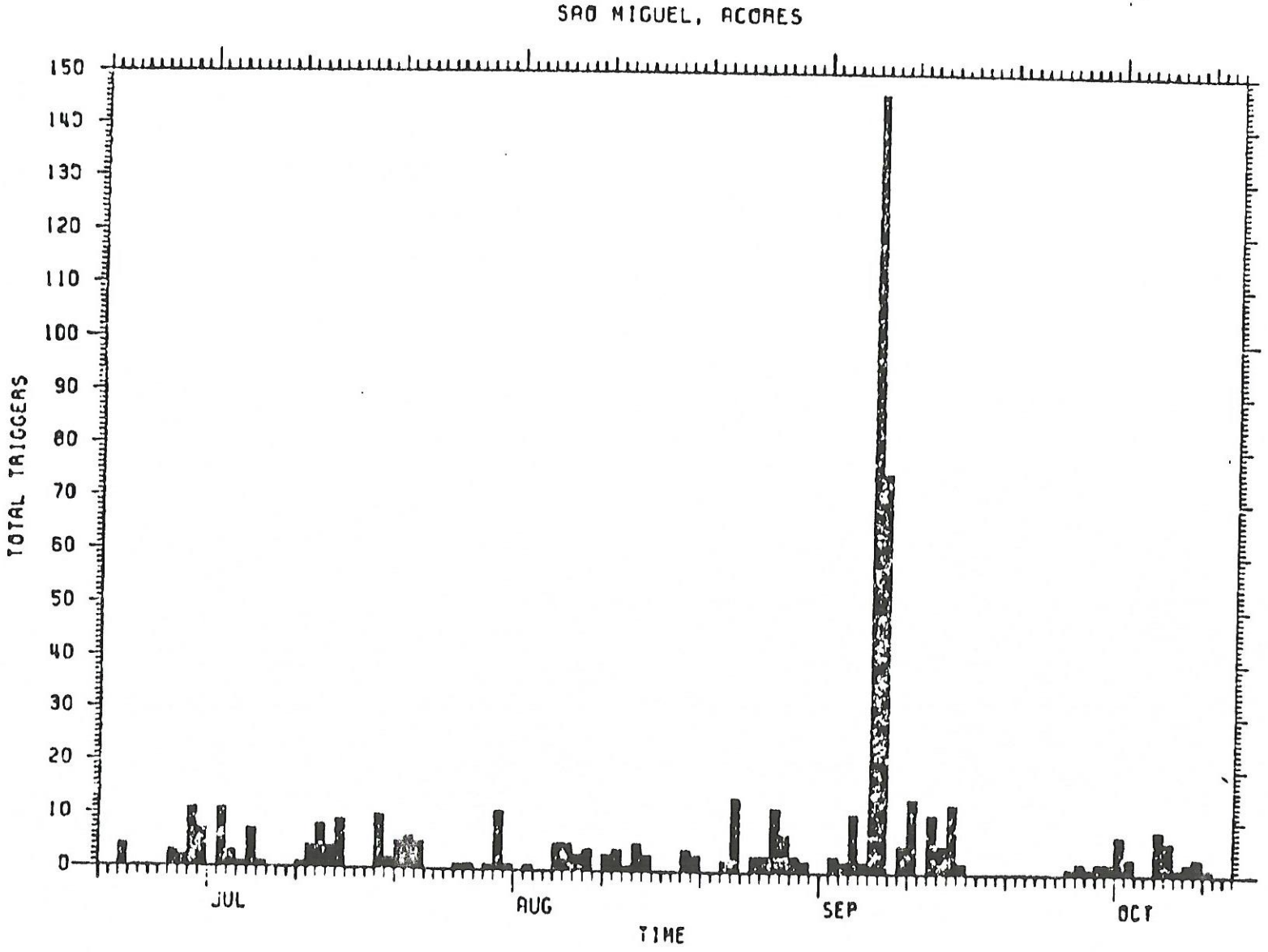

Figure 11. Total seismic triggers determined from analog playbacks of approximately 7500 station records.

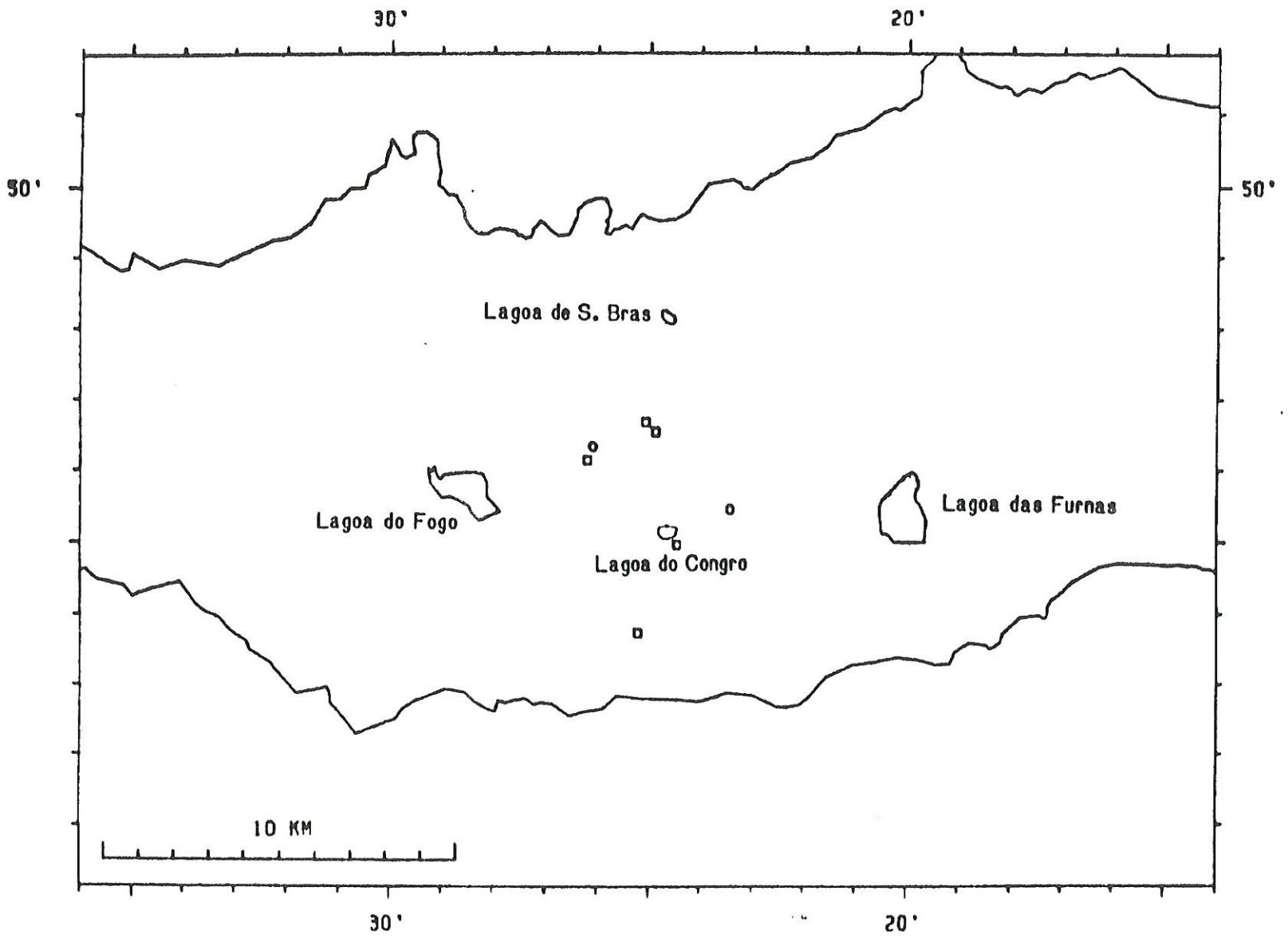

Figure 12. Epicentral locations of the events of June 28-29, 1983.

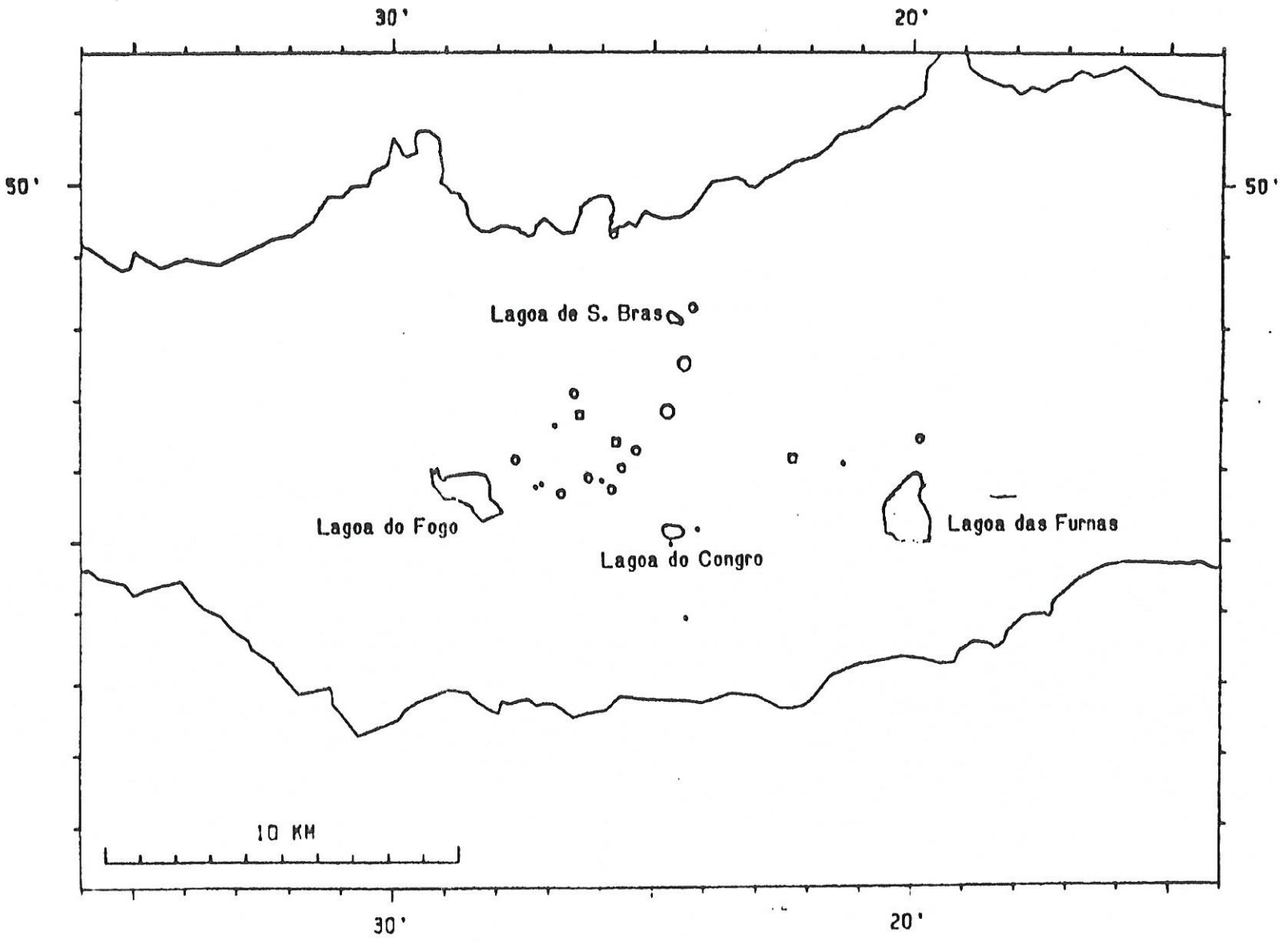

Figure 13. Epicentral locations of the events of September 6-7, 1983.

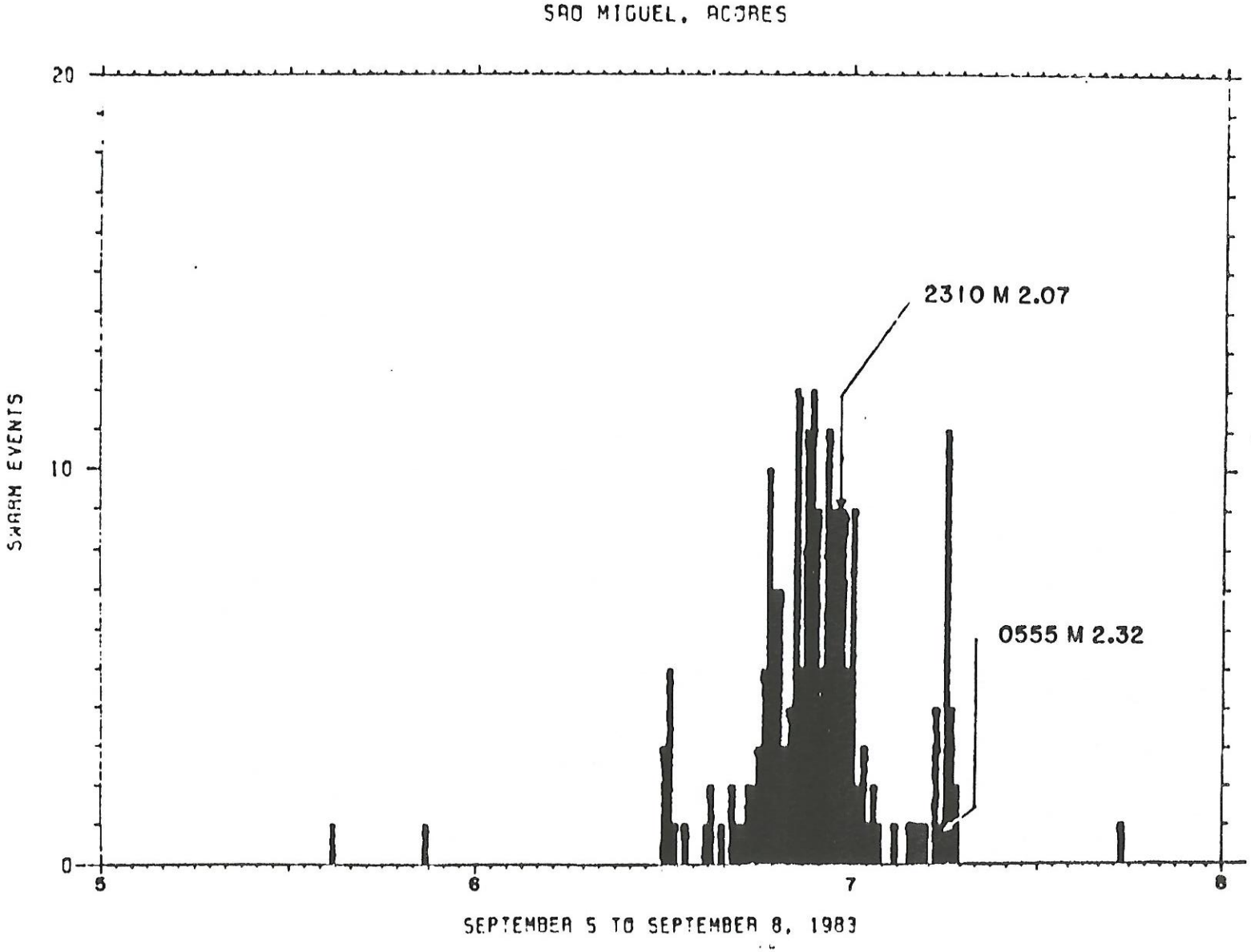

Figure 14. Single station and located events during the September 6-7, 1983 swarm.

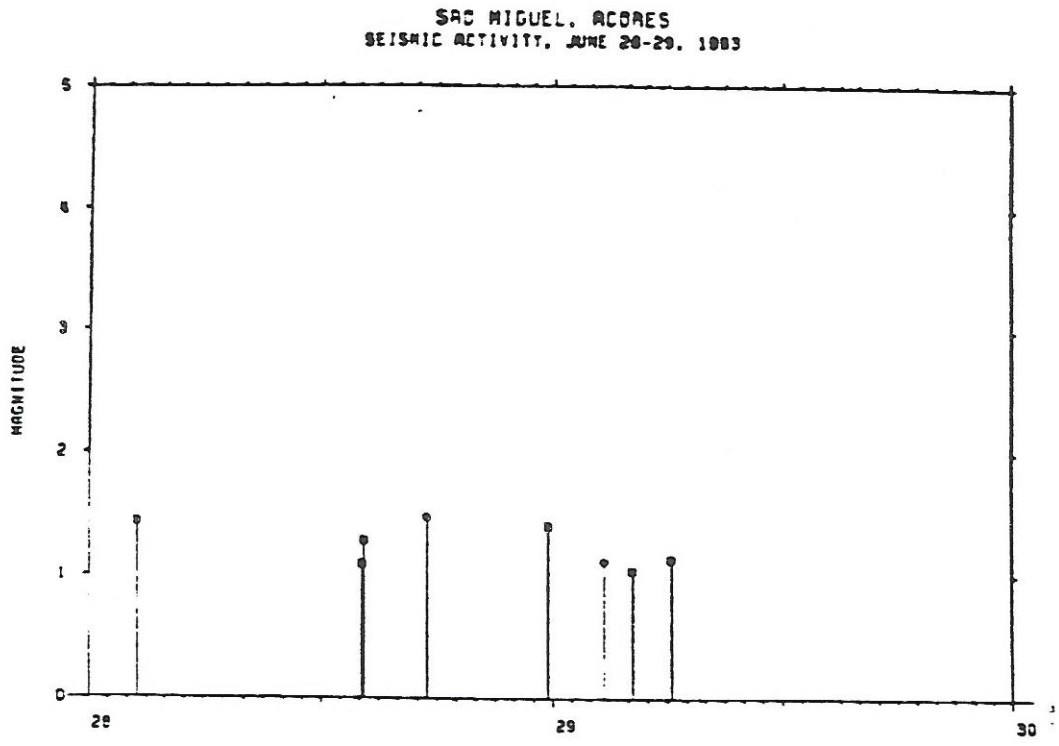

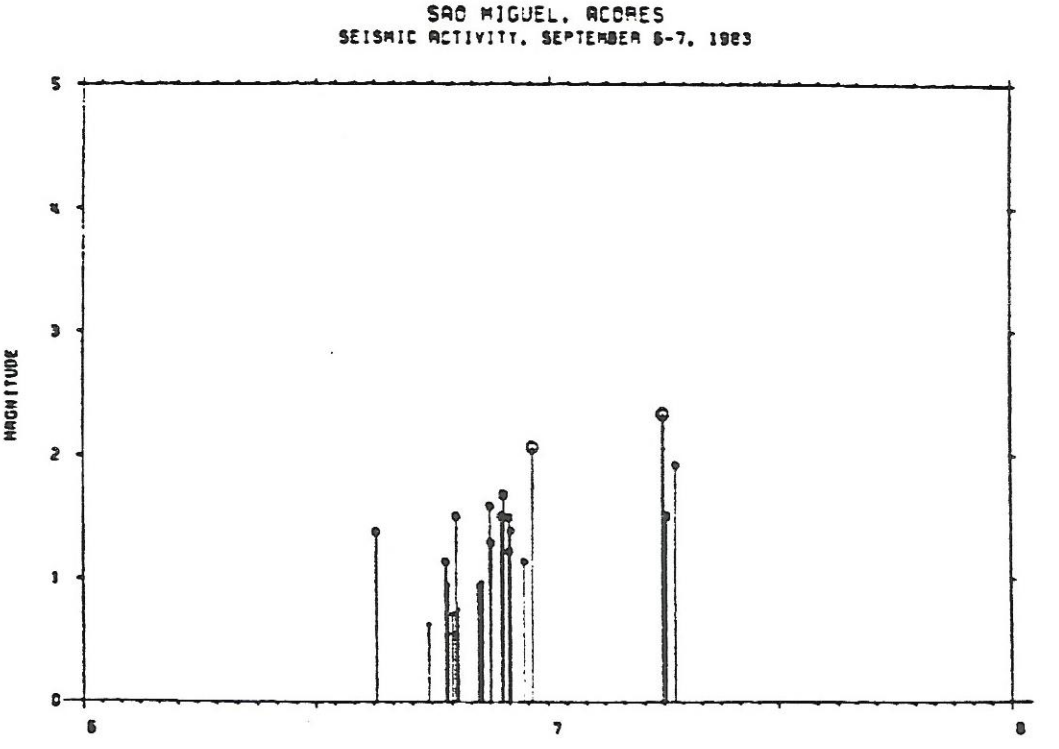

Figure 15. Magnitude versus time plots for the June and September, 1983 swarms.

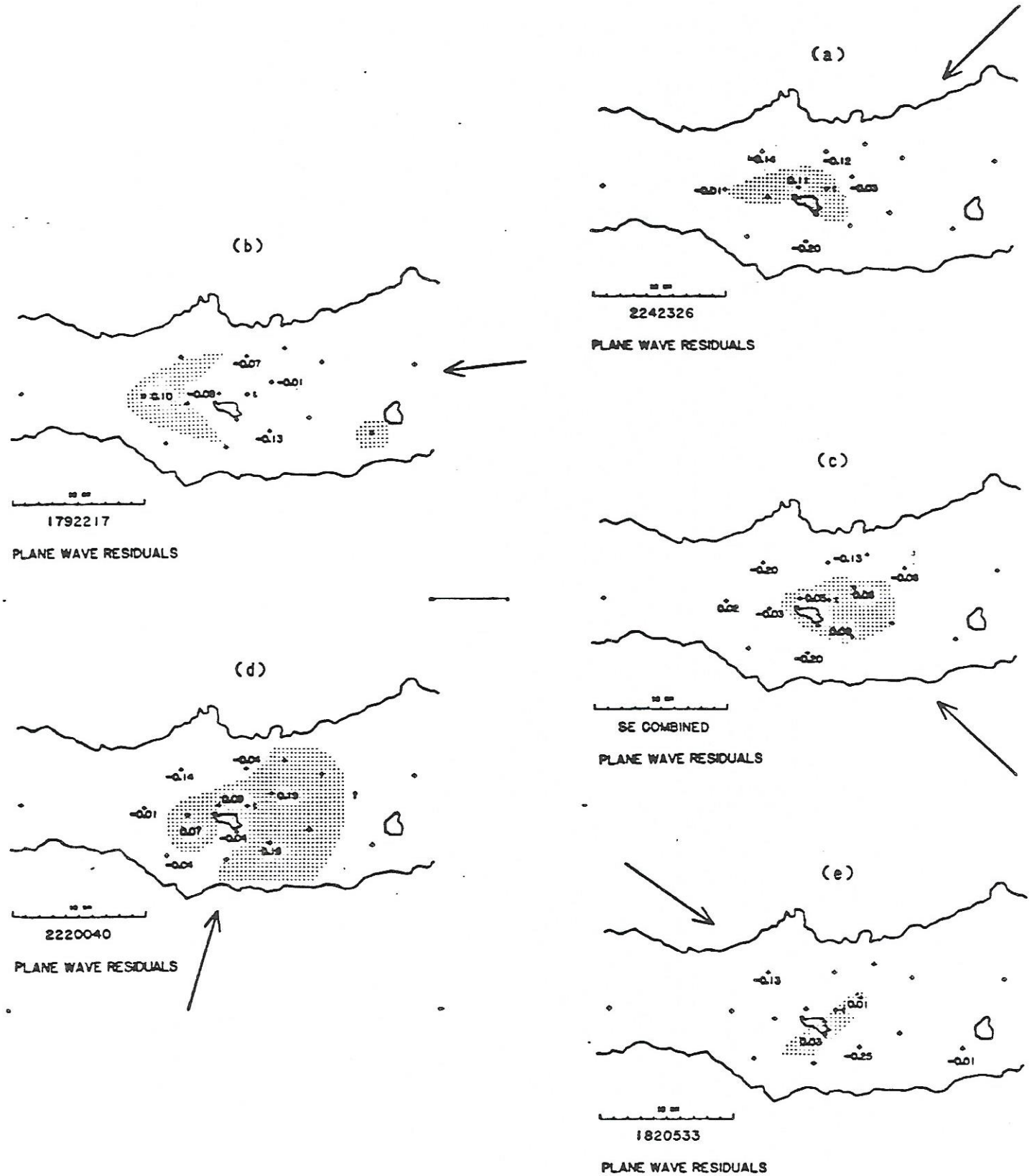

Figure 20. Residuals from the plane wave solution, high residuals are stipled.

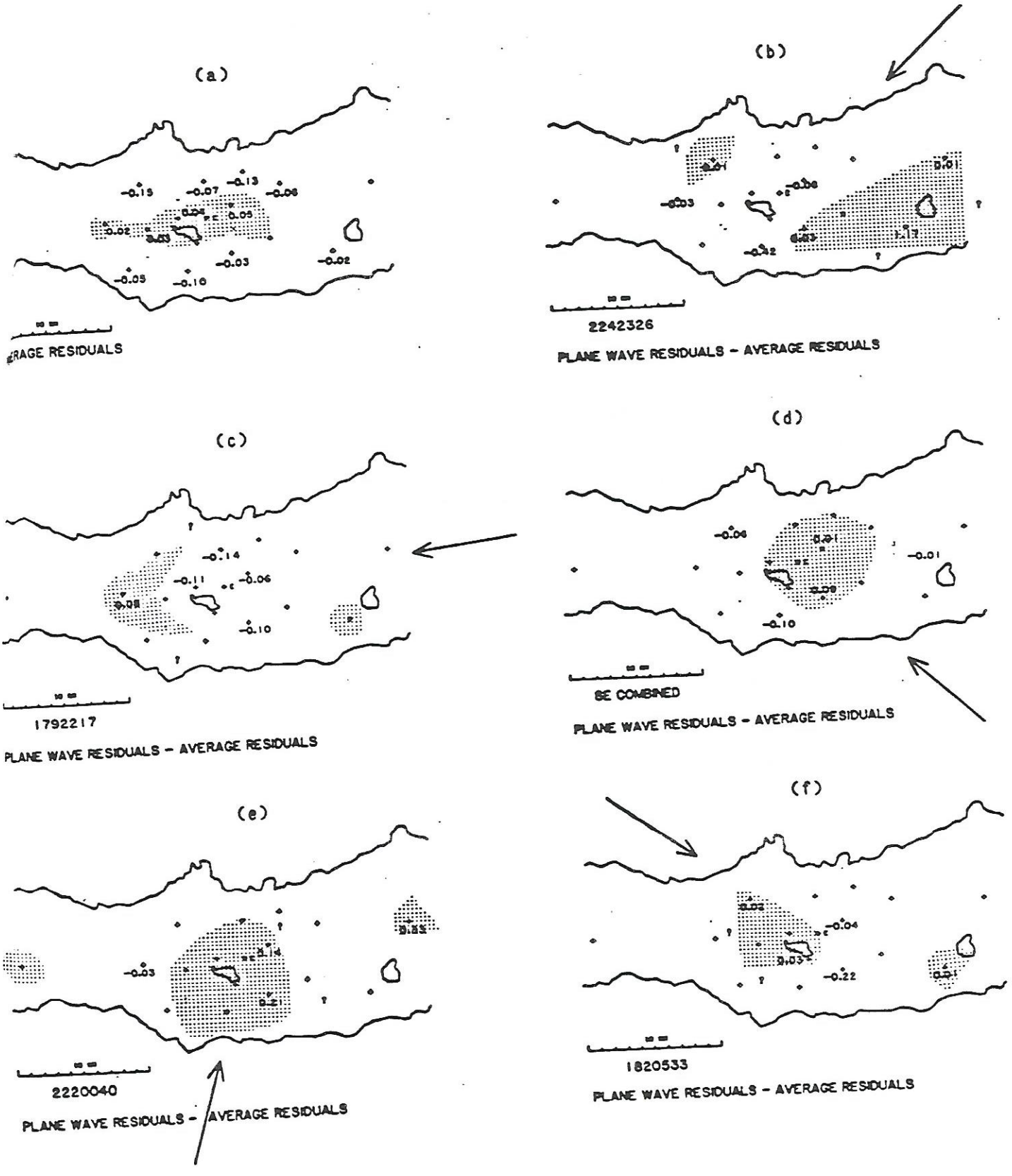

Figure 21. Figure 21a shows the average plane-wave residuals for the five regional events. 21b-f are plots of the average residuals subtracted from the plane-wave residuals for each event.

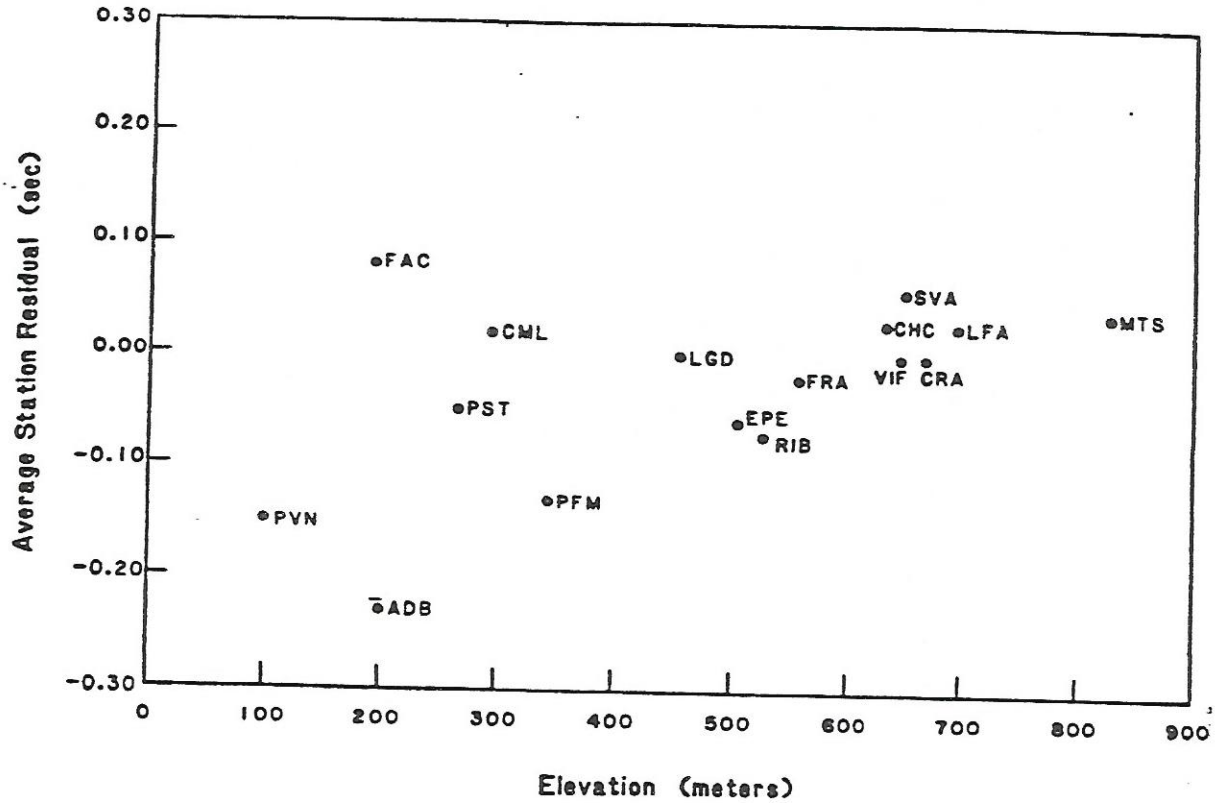

Figure 22. Average station residuals plotted against elevation. Note that except for FAC and CML, the approximate linear regression of the data indicating 0.2 km/sec delay for each kilometer of elevation increase.

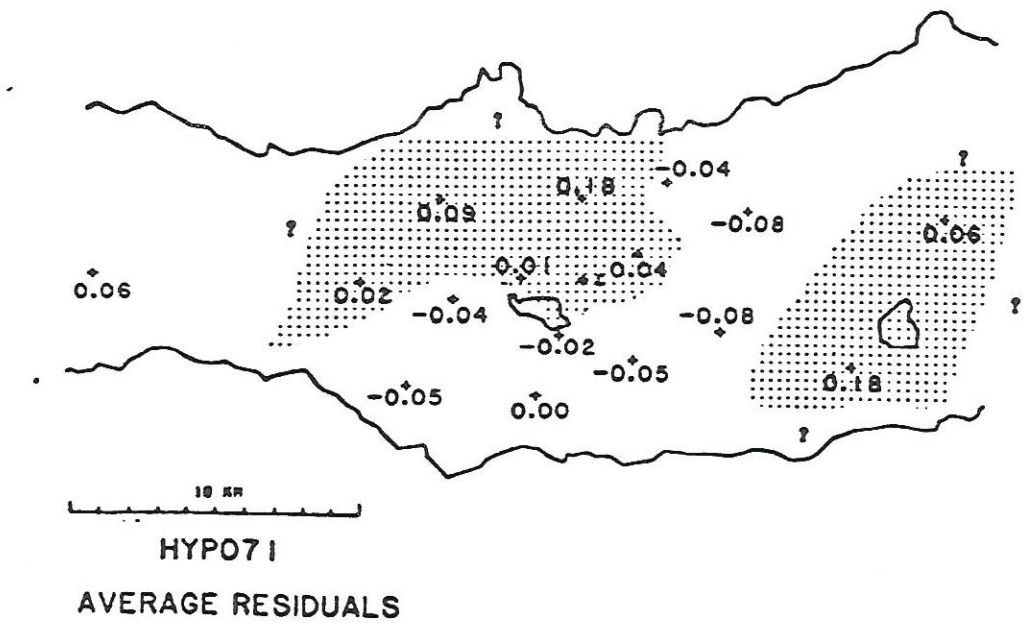

Figure 23. Average station residuals for the regional events from the HYPO71 output.